Journal of Pharmaceutical Sciences 108 (2019) 929-948

Contents lists available at ScienceDirect

Journal of Pharmaceutical Sciences

journal homepage: www.jpharmsci.org

Pharmaceutics, Drug Delivery and Pharmaceutical Technology

# Changes in the Solid State of Nicergoline, a Poorly Soluble Drug, Under Different Grinding and Environmental Conditions: Effect on Polymorphism and Dissolution

Roberta Censi, Maria Rosa Gigliobianco, Cristina Casadidio, Piera Di Martino*

*University of Camerino, School of Pharmacy, Via S. Agostino, Camerino, Italy*

ARTICLE INFO

*Article history:*
Received 18 April 2018
Revised 25 September 2018
Accepted 28 September 2018
Available online 6 October 2018

*Keywords:*
nicergoline
poorly water soluble drug
grinding
amorphous
polymorph
hydrate
dissolution

ABSTRACT

Nicergoline native crystals (Form I) were subjected to different grinding methods for 15, 30, 45, and 60 min: Method A, grinding at 20°C under air atmosphere; Method B, grinding in presence of liquid nitrogen under air atmosphere; Method C, grinding at 20°C under nitrogen atmosphere; and Method D, grinding in presence of liquid nitrogen under nitrogen atmosphere. Scanning electron microscopy, differential scanning calorimetry, X-ray powder diffractometry, thermogravimetry, and infrared spectroscopy were used to follow changes in the particle size and in crystalline structures. Batches from Methods A and C underwent partial amorphization immediately after grinding; Form II was obtained by heating these partially amorphous forms or after spontaneous crystallization after 1 and 5 months storage. Method B promoted the hydration of nicergoline to a monohydrate form. Batch D was stable under grinding and neither amorphization nor hydration were observed. The best intrinsic dissolution rate was that of metastable Form II, followed by Form I, while the worst was that of the Method B monohydrate form. The slowest particle dissolution was observed for hydrated particles, because of the lowest IDR, while the most rapid was exhibited by batch D, because of the very small particle size.



## Introduction

Nicergoline, a semisynthetic ergot derivative with potent blocking properties for α1-adrenoreceptors, is insoluble in water (0.002 mg $mL^{-1}$ at 25°C) in its crystalline commercial Form I.

Thus, the application and evaluation of all the methods and formulations able to improve the solubility and dissolution rate of nicergoline are of paramount importance.

Nicergoline exists in 2 different polymorphic forms which exhibit a monotropic relationship,[1] a triclinic Form I,[1,2] and a less thermodynamically stable orthorhombic Form II.[1,3,4] In a previous study, we highlighted differences in solubility and dissolution rates of these nicergoline polymorph Forms I and II,[1] and in this study we noted that their monotropic relationship explains the higher solubility of the metastable Form II.

Several studies seeking to improve the solubility and/or dissolution rate of nicergoline have been conducted. Our group has conducted 3 studies seeking to improve the solubility and/or dissolution rate of nicergoline. Dissolution studies of a solid dispersion of nicergoline in polyvinylpyrrolidone K30 (PVP K30) achieved improved particle dissolution rates[5] that were inferior only to the pure amorphous form.[6] Enhanced solubility and dissolution rates were also demonstrated for nicergoline nanoparticles obtained by a nanospray drying method: the small particle size combined with the amorphous state of nicergoline was responsible for increased solubility and particle dissolution.[7]

Thus, the objective of this study was to apply to nicergoline another technique, cryo-milling, known to efficiently decrease particle size and thus dissolution rate, and to evaluate its effectiveness in enhancing particle size reduction and particle dissolution as well as to assess the impact of this technique on the physicochemical stability of the drug.

Currently, in order to improve the bioavailability of poorly soluble drugs, pharmaceutical firms still rely most frequently on particle size reduction, generally achieved by mechanical methods,[8-10] which according to the Noyes and Whitney law promotes an increase in dissolution rate through an increase in drug surface area in contact with dissolution media.

The traditional size of pharmaceutical powders, generally ranging from a few hundred microns up to 50 μm, sometimes fails to provide an appropriate drug dissolution rate, and thus micronization is frequently necessary.[11] Ball mills and jet mills have long been used for micronization[12] to reduce particle size, generally to the range of 10-30 μm.

* *Correspondence to:* Piera Di Martino (Telephone: +39-0737-402215).
*E-mail address:* piera.dimartino@unicam.it (P. Di Martino).

https://doi.org/10.1016/j.xphs.2018.09.032
0022-3549/

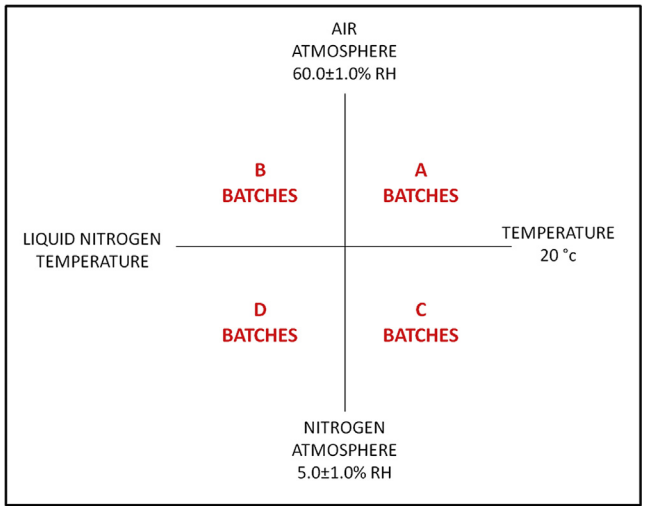


**Figure 1.** Depiction of the experimental conditions used to produce batches A, B, C, and D

Additionally, cryo-milling, which consists in grinding particles at temperatures below room temperature, has proven to be a very simple and effective technique for reducing drug particle size to micrometric or even submicron ranges, thus improving particle dissolution rates.[13-17] However, some researchers have reservations about grinding because it may induce unwanted reactions in the drug, affecting its physicochemical stability.[18-20] Even so, grinding and in particular grinding at different temperatures has emerged as a mechanochemical method for screening new pharmaceutical solid forms.[21-23]

To summarize, the objectives of this study were to:

(1) Improve the dissolution rate of nicergoline, a poorly soluble drug, by grinding under different conditions to reduce its particle size;
(2) Verify the physicochemical stability of ground particles.

In the present study, nicergoline Form I native crystals were subjected to 4 grinding conditions:

Method A: Grinding at 20°C under air atmosphere; Method B: Grinding in presence of liquid nitrogen under air atmosphere;

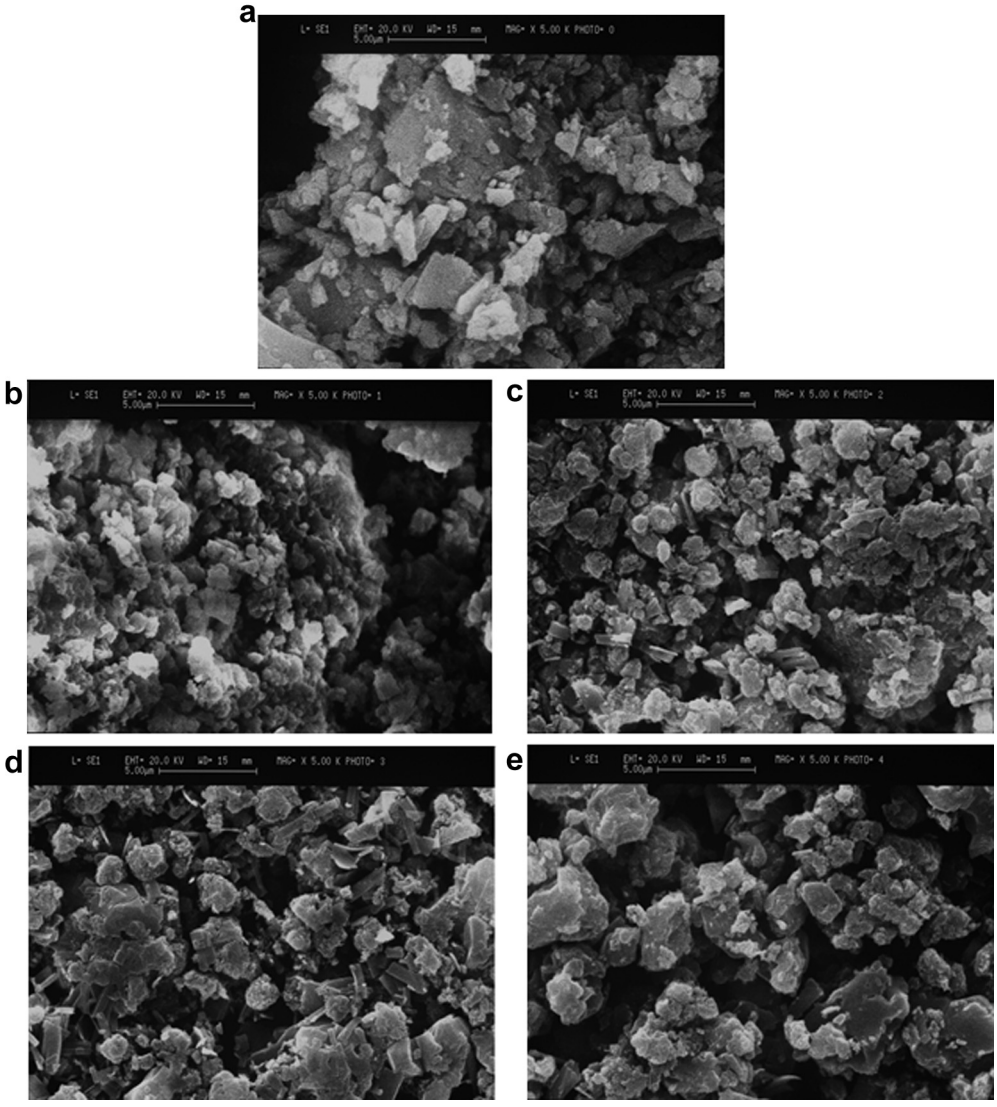


**Figure 2.** Scanning electron photomicrographs of nicergoline crystals ground under Method A: 20°C under air atmosphere (60.0 ± 1.0% RH). Native Crystals (a), Batch A-15 (b), Batch A-30 (c), Batch A-45 (d) and Batch A-60 (e). Magnification of 5000 ×.

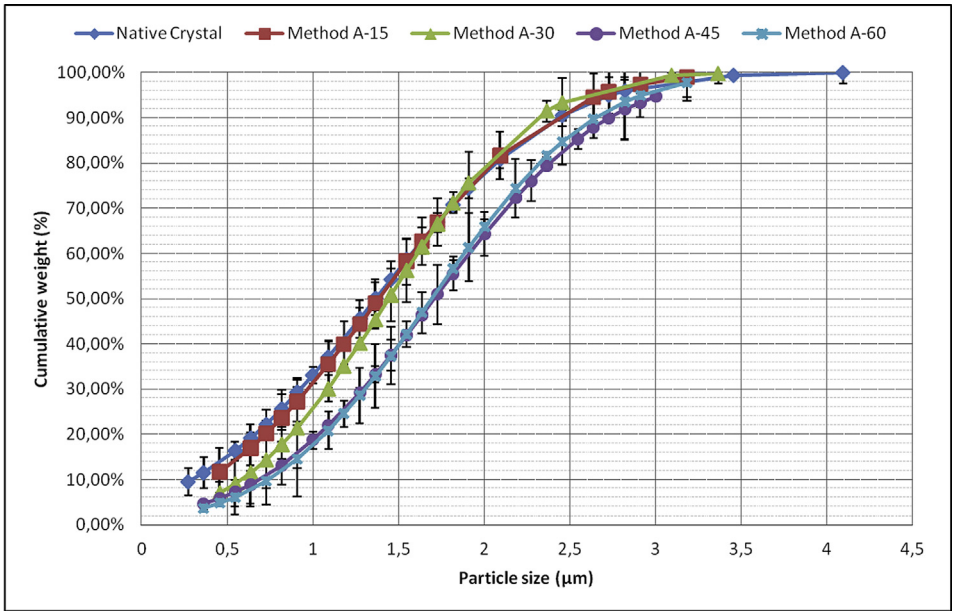


**Figure 3.** Particle size distribution profile of nicergoline crystals ground under Method A: 20°C under air atmosphere (60.0 ± 1.0% RH). Standard Deviations are indicated.

Method C: Grinding at 20°C under nitrogen atmosphere; and Method D: Grinding in presence of liquid nitrogen under nitrogen atmosphere.

## Materials and Methods

### *Materials*

One batch of nicergoline (NIC) (Form I) was purchased from China-Japan Shandong Hongfuda Pharmchem Co., Ltd., (Shandong, China) as white crystalline powder and used as received for further analyses and experiments. It was stored in a desiccator in tightly closed glass vials (25°C ± 2°C, 2.0 ± 0.1 relative humidity [RH]%). NIC is referred to as native crystals (NCs) in the text when it was not subjected to grinding. Nicergoline is physicochemically stable under normal conditions of use.

Nicergoline Form II was obtained according to the method of Malaj et al.[1] Briefly, an excess of nicergoline, able to form a saturated solution at room temperature, was completely dissolved in tetrahydrofuran (THF) (Sigma-Aldrich, Stenheim, Germany) at 40.0°C ± 0.5°C, and the solution was then cooled at 10°C under continuous stirring, by means of an external ethanol cooling system (Cryostat F4-Q; Haake Q, Karlsruhe, Germany). Crystals were recovered by vacuum filtration, dried at room temperature for 24 h in a ventilated oven, then stored in a desiccator in tightly closed glass vials (25°C ± 2°C, 2.0 ± 0.1 RH%). Crystals were used as obtained without any further treatment.

Amorphous nicergoline was obtained according to Martena et al.[6] Briefly, NIC was dissolved in chloroform and solvent was evaporated under reduced pressure at 25°C. The residual solvent was removed under vacuum in the presence of liquid nitrogen. The viscous amorphous NIC was stored for approximately 24 h at a temperature lower than the glass transition temperature to obtain a solid amorphous form, which was then ground for use.

### *Grinding Procedures*

One gram of NCs was manually ground with a ceramic pestle in a 500-mL ceramic mortar for 60 min at 20°C and 60.0 ± 1.0% RH. During the 60-min grinding, several samples were withdrawn from the mortar (after 15, 30, 45, and 60 min) giving rise to 4 different batches according to the length of grinding time (A-15, A-30, A-45, and A-60). The same procedure was applied by adding liquid nitrogen (purity 99.999%, water content <0.05 ppm; Air Liquide Italy, Milan, Italy) to the mortar directly in contact with the powder and refilling liquid nitrogen during grinding (Method B). This procedure gave rise to the following batches: B-15, B-30, B-45, and B-60. Both grinding procedures were also carried out either under air atmosphere (60.0 ± 1.0% RH) or under nitrogen atmosphere, realized by saturating the closed mortar with gaseous nitrogen (5.0 ± 1.0% RH).

Thus, in more detail, the grinding conditions used were as follows:

(1) Method A: Grinding at 20°C under air atmosphere (60.0 ± 1.0% RH) (Batches A-15, A-30, A-45, A-60).
(2) Method B: Grinding in presence of liquid nitrogen under air atmosphere (60.0 ± 1.0% RH) (Batches B-15, B-30, B-45, B-60).
(3) Method C: Grinding at 20°C under nitrogen atmosphere (5.0 ± 1.0% RH) (Batches C-15, C-30, C-45, C-60).
(4) Method D: Grinding in presence of liquid nitrogen under nitrogen atmosphere (5.0 ± 1.0% RH) (Batches D-15, D-30, D-45, D-60).

As a help to the reader, Figure 1 depicts the experimental conditions used to produce the different batches.

Immediately after grinding and before each analysis, to prevent any further contact with humidity, ground samples were stored in a desiccator in tightly closed glass vials (25°C ± 2°C, 2.0 ± 0.1 RH%). All the grinding procedures were repeated 3 times to assess the repeatability of results. Batches were not sieved. No batch-to-batch variability was observed and results were always highly reproducible. Because no batch-to-batch variability was observed for the same grinding procedure, results presented in this work correspond to the analyses repeated on the same batch.

### *Differential Scanning Calorimetry Analysis*

Differential scanning calorimetry (DSC) analysis was performed on a Pyris 1 (Perkin Elmer, Co., Norwalk, CT) equipped with a

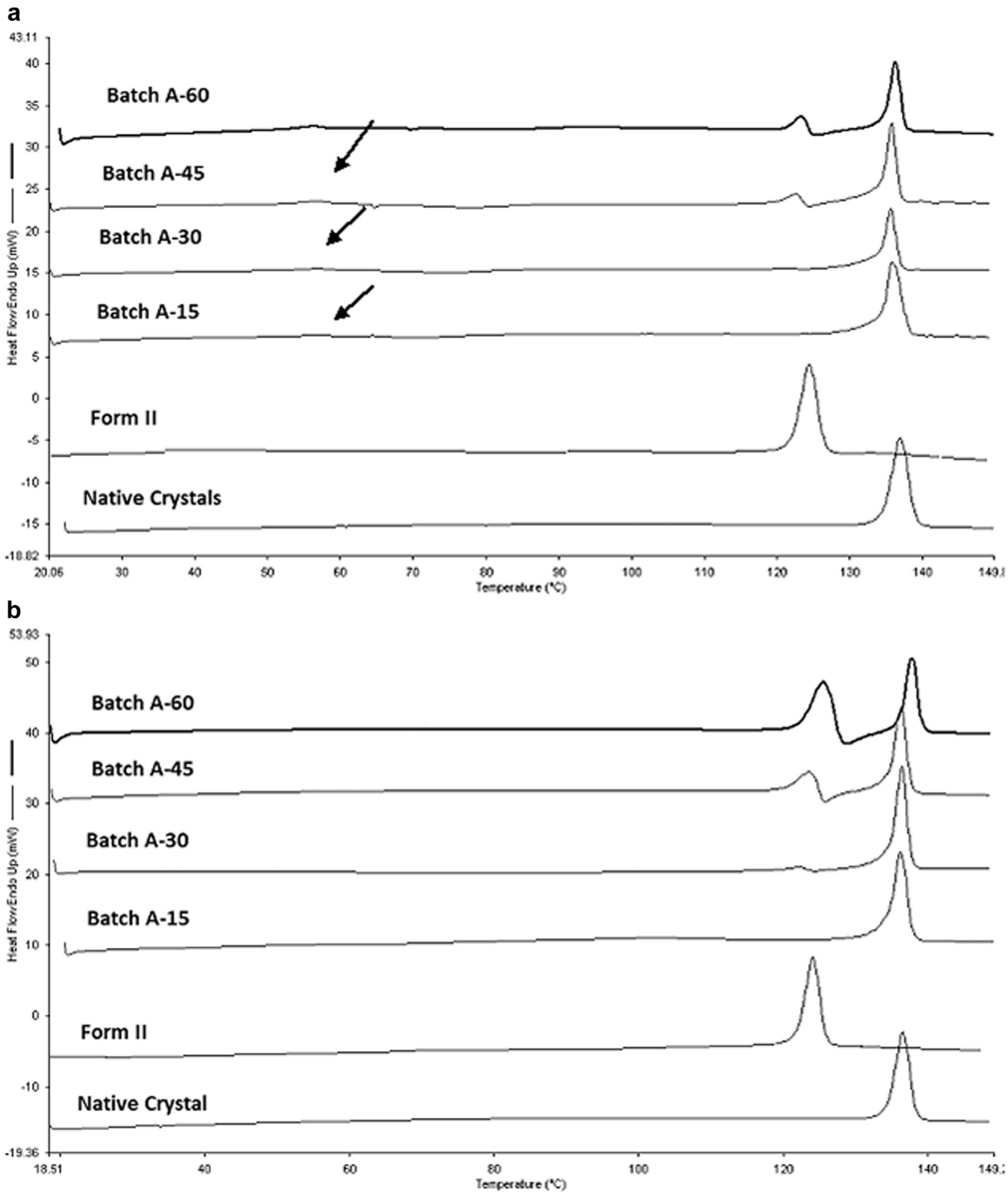


**Figure 4.** Differential scanning calorimetry thermograms of nicergoline ground under Method A: 20°C under air atmosphere (60.0 ± 1.0% RH). (a) Analysis run immediately after grinding. (b) Analysis run 5 mo after grinding. Arrows highlight glass transition.

cooling device (Intracooler 2P, Cooling Accessory; Perkin Elmer Co.). A dry purge of nitrogen gas (20 mL $min^{-1}$) was used for all runs. DSC was calibrated for temperature and heat flow using a pure sample of indium and zinc standards. Sample mass was about 4-5 mg and perforated aluminum pans of 50 μL were used.

DSC was used to determine the onset melting temperature ($T_m$) and glass transition temperature. The latter was characterized for

**Table 1**
Physicochemical Characterization of Nicergoline Batches Ground Under Method A

| Characteristic | Glass Transition | | Form II Melting | | Form I Melting | | Relative Crystallinity Degree | Water Loss |
|---|---|---|---|---|---|---|---|---|
| | $T_g$ °C | ΔCp J/Kg* °C | $T_m$ °C | ΔH J/g | $T_m$ °C | ΔH J/g | % | % W/W |
| NCs Form I | – | – | – | – | 134.56 ± 0.67 | 63.10 ± 2.54 | 100 | 0.15 ± 0.01 |
| Form II | – | – | 120.34 ± 1.16 | 55.28 ± 1.24 | – | – | 100 | 0.35 ± 1.18 |
| Analyzed immediately | | | | | | | | |
| A-15 | – | – | – | – | 134.20 ± 1.08 | 50.09 ± 2.67 | 92 | 0.12 ± 0.01 |
| A-30 | 52.89 ± 0.79 | 490 ± 30 | 118.85 ± 1.73 | 0.64 ± 1.34 | 134.04 ± 1.15 | 44.30 ± 1.79 | 55 | 0.15 ± 0.01 |
| A-45 | 52.53 ± 0.88 | 470 ± 50 | 119.83 ± 0.98 | 6.27 ± 2.03 | 134.26 ± 0.74 | 42.32 ± 1.28 | 34 | 0.13 ± 0.02 |
| A-60 | 51.53 ± 0.10 | 520 ± 50 | 121.05 ± 1.02 | 8.13 ± 2.57 | 134.68 ± 0.55 | 42.24 ± 0.78 | 12 | 0.13 ± 0.01 |
| Analyzed after 5 mo | | | | | | | | |
| A-15 | – | – | – | – | 134.33 ± 1.28 | 56.27 ± 1.23 | 97 | 0.15 ± 0.02 |
| A-30 | – | – | 123.52 ± 1.14 | 1.59 ± 1.56 | 134.82 ± 1.32 | 51.24 ± 1.15 | 97 | 0.15 ± 0.01 |
| A-45 | – | – | 120.34 ± 1.25 | 15.01 ± 1.03 | 134.65 ± 0.87 | 49.46 ± 1.24 | 100 | 0.16 ± 0.01 |
| A-60 | – | – | 122.33 ± 1.43 | 35.80 ± 1.67 | 136.00 ± 0.96 | 33.68 ± 0.76 | 100 | 0.15 ± 0.02 |

The extrapolated onset temperature ($T_m$) and the melting enthalpy were determined by DSC.
Relative crystallinity degree was determined by XRPD, and the water content % by TGA. Values are the mean of 3 measurements, and standard deviations are indicated.

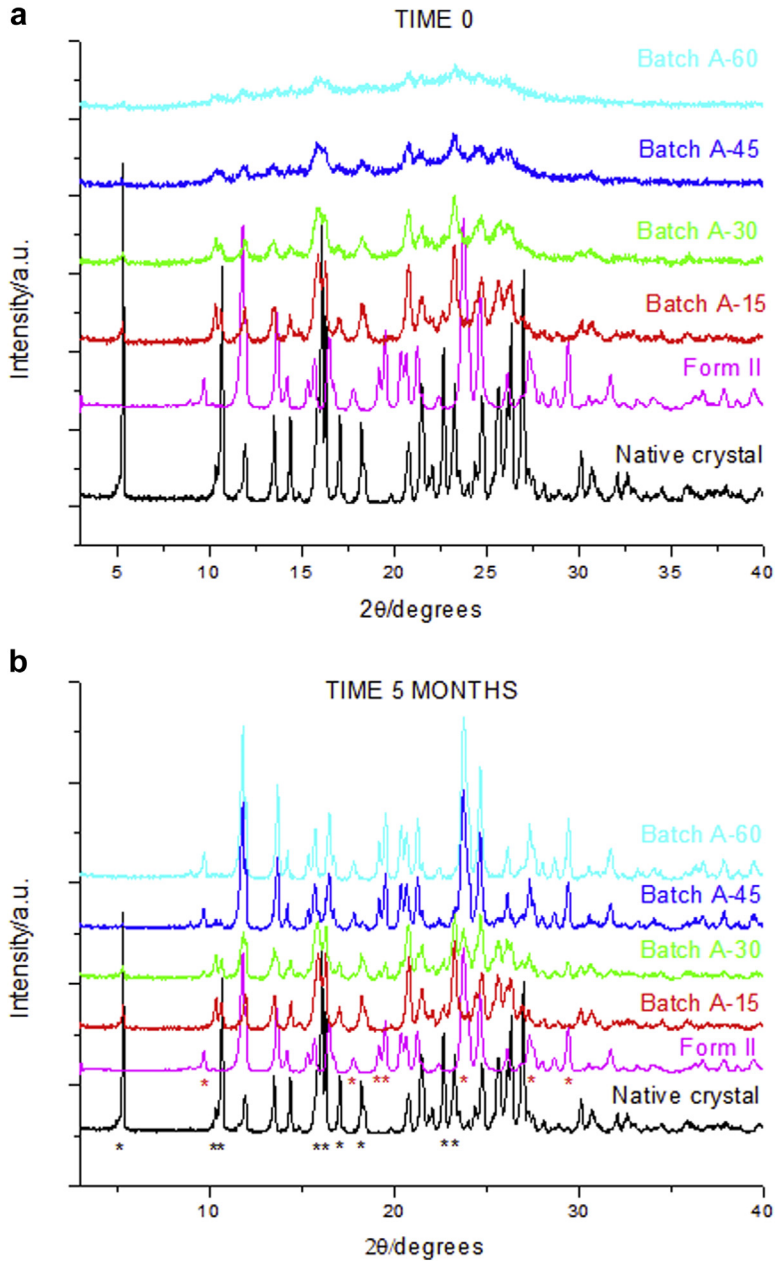


**Figure 5.** X-ray powder diffraction patterns of nicergoline ground under Method A: 20°C under air atmosphere (60.0 ± 1.0% RH). (a) Analyses performed immediately after grinding. (b) Analyses performed after 5 mo.

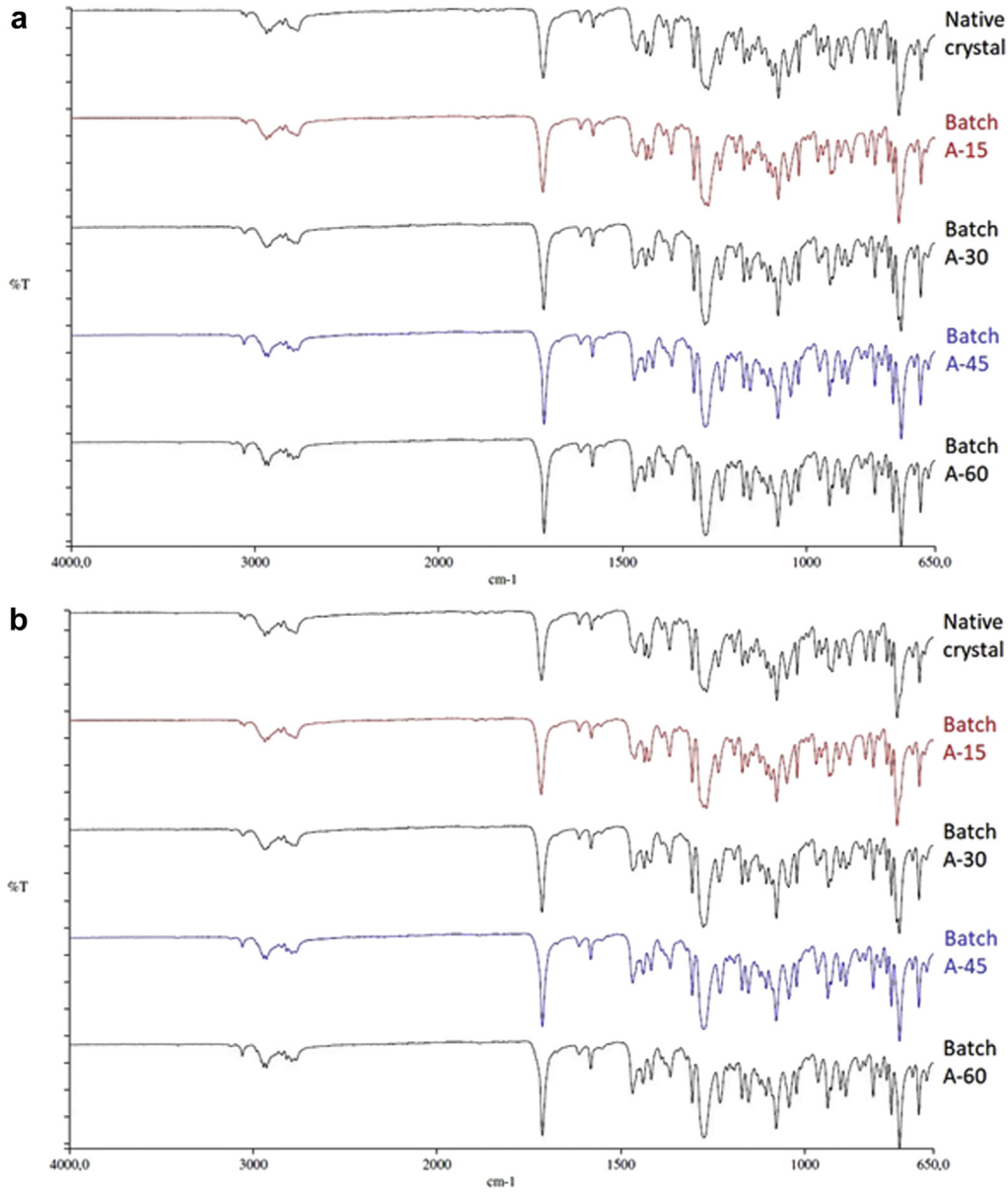


**Figure 6.** Infrared spectroscopy of nicergoline ground under Method A: 20°C under air atmosphere (60.0 ± 1.0% RH). (a) Analyses performed immediately after grinding. (b) Analyses performed after 5 mo.

temperature ($T_g$) and change in heat capacity ($\Delta C_p$), and measurements were carried out at a heating rate of 10°C $min^{-1}$.

*Thermogravimetric Analysis*

Thermogravimetric analysis was performed on a Pyris 1 TGA (Perkin Elmer, Co.) in 0.07 mL open aluminum oxide pans, with a sample mass of 4-5 mg, and at a scanning rate of 10°C $min^{-1}$. A dry purge of nitrogen gas (20 mL $min^{-1}$) was used for all runs. TGA was calibrated for temperature and heat flow using pure standards of alumel, nickel, perkalloy, and iron. Calibration was repeatedly checked to assure deviation $\leq \pm 0.3$°C.

*X-Ray Powder Diffractometry*

X-ray powder diffractometry (XRPD) was used to assess the solid state of the studied samples and to evaluate their physical stability under grinding. To this end, a Philips PW 1730 (Philips Electronic Instruments Corp., Mahwah, NJ) was used as an X-ray generator for Cu Kα radiation ($\lambda_{\alpha 1} = 1.54056$ Å, $\lambda_{\alpha 2} = 1.54430$ Å). The experimental X-ray powder patterns were recorded on a Philips PH 8203. The goniometer supply was a Philips PW 1373 and the channel control was a Philips PW 1390. Data were collected in the discontinuous scan mode using a step size of 0.01° 2α. The scanned range was 2 θ to 40° (2 θ).

The relative crystallinity degree of powders was evaluated by XRD and calculated according to a previously described method.[24] Briefly, a calibration curve was determined from physical mixtures of completely crystalline NIC (100% crystalline) and completely amorphous NIC (100% amorphous). For the 100% crystalline fraction, we selected the Native Crystals Form I assuming it as 100% crystalline, because no other reference materials exist, while the completely amorphous form was confirmed by XRPD. Thus, the term "relative" crystallinity degree refers to the real samples used for the determination. The calibration curve of physical mixtures was determined, in presence of an internal standard, by calculating

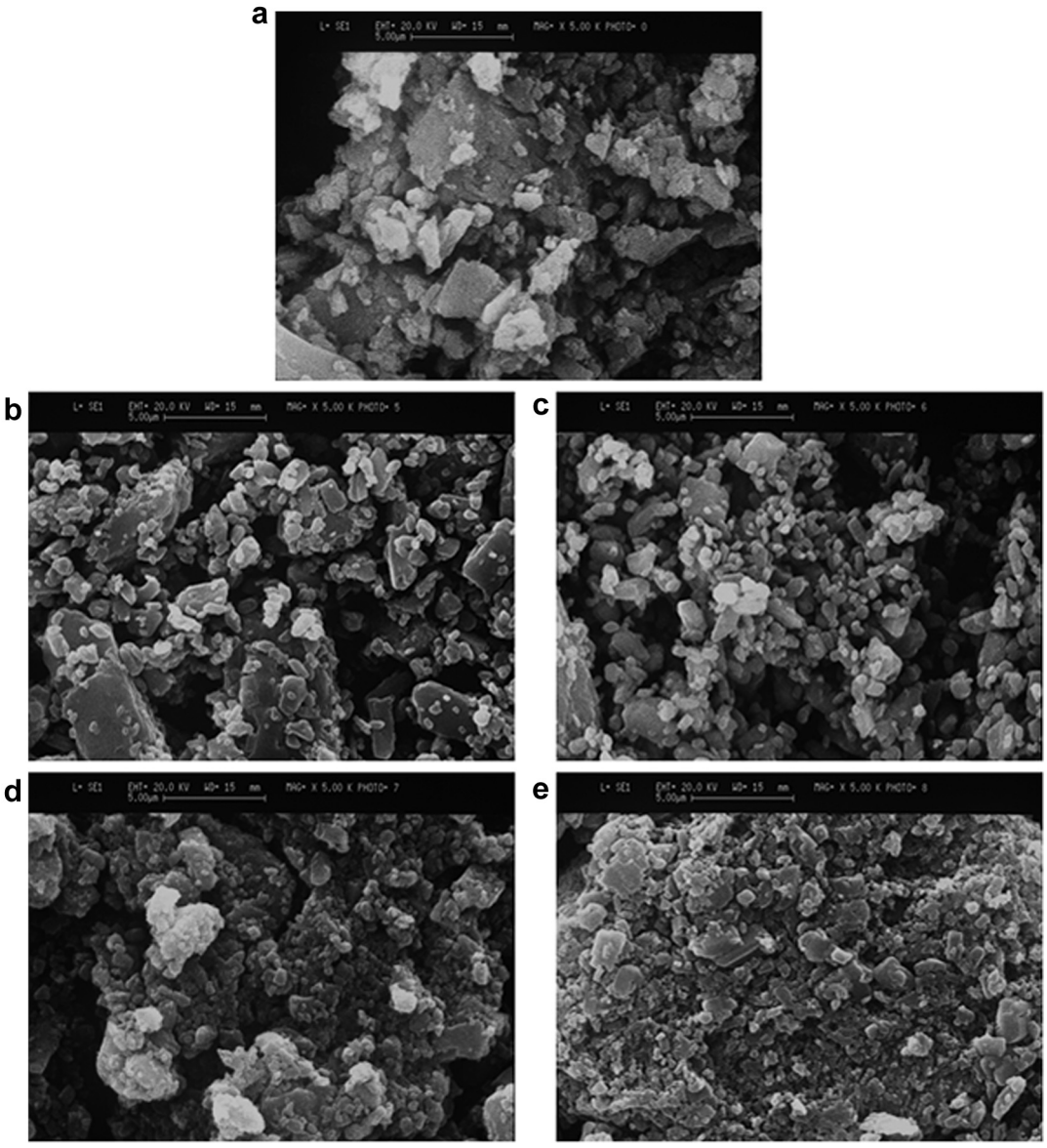


**Figure 7.** Scanning electron photomicrographs of nicergoline crystals ground under Method B: in presence of liquid nitrogen and air atmosphere (60.0 ± 1.0% RH). Native Crystals (a), Batch B-15 (b), Batch B-30 (c), Batch B-45 (d) and Batch B-60 (e). Magnification of 5000 ×.

the total area ($A_{tot}$) of the diffraction patterns (crystalline + amorphous) and the area ($A_{Cr}$) of the crystalline part (the area over the peak baseline). The powder crystallinity degree was expressed according to the following Equation 1:

$$Crystallinity\ (\%) = \frac{A_{Cr}}{A_{tot}} \cdot 100 \quad (1)$$

The crystallinity degree was the average value of 3 different measurements. The statistical significance was evaluated by a 1-way analysis of variance test for $\alpha = 0.05$.

*Scanning Electron Microscopy*

NIC crystal morphology was determined using 2 different scanning electron microscopes (SEM): a Stereoscan 360 (Cambridge Instruments, Cambridge, UK) and a Field Emission Scanning Electron Microscope (FE-SEM) (Sigma 300; Carl Zeiss Microscopy GmbH, Jena, Germany). In both cases, samples were mounted on a metal stub with double-sided adhesive tape and then sputtered under vacuum with a gold layer, in the case of the first microscope (Balzer MED 010; Linchestein), or a chromium layer, in the case of the second one (Q150T; Quorum Technologies Ltd., Lewes, UK).

The particle size of nicergoline powder samples was determined by measuring the mean Feret diameter of 500 particles using the MagniSci Software (Toronto, Canada). Particle size (μm) was expressed as cumulative weight percentage and standard deviations were provided.

*Infrared Spectroscopy*

Infrared spectroscopy was performed on a Spectrum 100 Fourier transform infrared spectrometer (Perkin Elmer, Co.).

*Long-Term Stability Studies*

The long-term stability study (1-5 months) was carried out by storing samples in tightly closed glass containers at 25°C ± 2°C in a

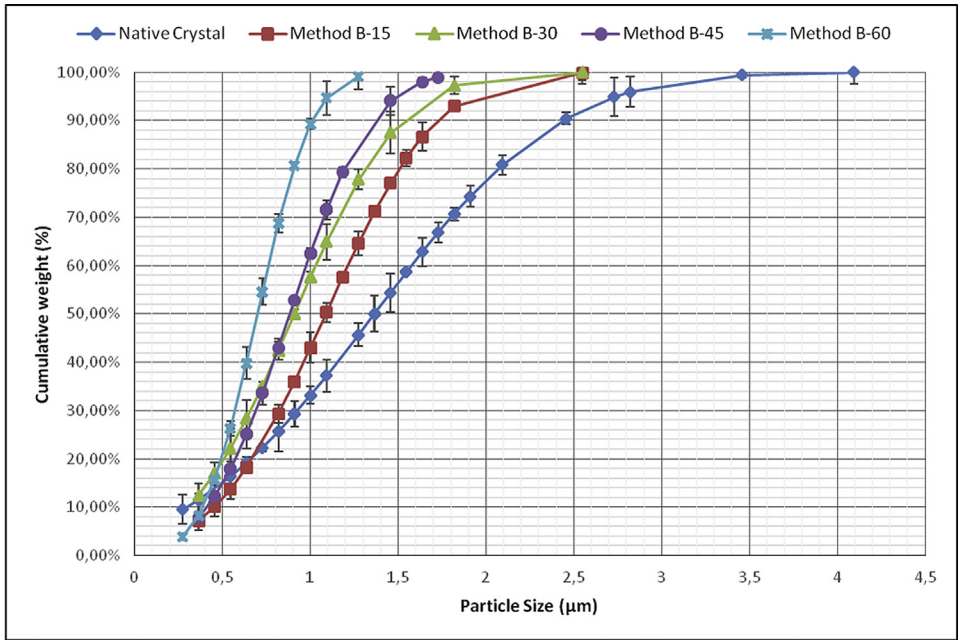


**Figure 8.** Particle size distribution profile of nicergoline ground under Method B: in presence of liquid nitrogen and air atmosphere (60.0 ± 1.0% RH). Standard deviations are indicated.

desiccator (2.0 ± 0.1 RH%) in order to avoid the effect of any possible humidity. The physical stability was evaluated by DSC, XRPD, and IR in order to assess possible changes in the physical solid form.

*Intrinsic Dissolution Rate Study*

The dissolution study was carried out by the rotating disk method.[25] Thirteen-millimeter-diameter tablets were obtained by compressing 300 mg of powder in a Perkin-Elmer hydraulic press for IR spectroscopy KBr disks, at a force of 15 kN for 10 min. This process yielded tablets with a surface area of 132.73 $mm^2$ that would not disintegrate during the test. Tablets were inserted into a stainless steel holder, so that only one face was exposed to the dissolution medium. The holder was then connected to the stirring motor of a dissolution apparatus (Erweka DT6, Gloucestershire, UK), centrally immersed in a 1000-mL beaker containing 900 mL of HCl 0.1 N at 37°C and rotated at 50 rpm. Suitable aliquots were withdrawn with a regenerated cellulose filter syringe at specified times and spectrophotometrically assayed for drug content at a wavelength of 288 nm (Agilent/HP 8453 UV-VIS Spectrophotometer; Agilent, San Diego, CA). A correction was calculated for cumulative dilution caused by replacement of the sample with an equal volume of original medium. Each test was repeated 6 times. Low standard deviations were obtained, indicating the good reproducibility of this technique. The intrinsic dissolution rates (IDR) were calculated from the slope of the straight line of cumulative drug release. Straight lines were selected adjusting R-squares, by using Origin® software (version 8.5) (Northampton, MA).

*Particle Dissolution*

Particle dissolution was carried out in a 1000-mL beaker containing 800 mL of HCl 0.1 N at 37°C and 0.5% of sodium laureth sulfate as surfactant and rotated at 50 rpm. Sink conditions were assured during the experiments. Suitable aliquots were withdrawn with a regenerated cellulose filter syringe at specified times and spectrophotometrically assayed for drug content at a wavelength of 288 nm (Agilent/HP 8453 UV-VIS Spectrophotometer). A correction was calculated for cumulative dilution caused by replacement of the sample with an equal volume of original medium. Each test was repeated 6 times. Low standard deviations were obtained, indicating the good reproducibility of this technique.

*Statistical Analysis*

Data were analyzed by 1-way analysis of variance, using a Bonferroni test. The statistical analysis was conducted using an Origin® software (version 8.5). Results are shown as mean ± SD and considered significantly different when $p < 0.05$.

## Results and Discussion

*Physicochemical Characterization of Nicergoline Nanoparticles*

*Method A: Grinding at 20°C Under Air Atmosphere (60.0 ± 1.0% RH)*

NCs appear as irregular particles with sharp, almost agglomerated edges (Fig. 2). Microphotographs of NCs subjected to grinding under Method A are shown in Figure 2. After 15 min of grinding, particles appeared smaller and more rounded than NCs, and a remarkable tendency to agglomeration was observed. As grinding proceeded, no further significant decrease in particle size was observed, while the tendency to agglomeration was still evident. In Figure 3, showing cumulative weight % versus particle size, the decrease in particle size as a consequence of grinding is poorly appreciable: a slight decrease in particle size can be noticed for Batches A-15, A-30, A-45, and A-60, all the corresponding curves being practically superimposed. In particular, the 50% cumulative weight was 1.72 µm for NCs, while nearly 1.35-1.40 µm for the other batches. Figure 4a shows the results of the DSC analysis run immediately after grinding. The curve of the NCs only showed an endothermic peak corresponding to the melting of Form I (Table 1) at 134.56°C ± 0.67°C. After 30 min of grinding, and more evidently after 45 and 60 min of grinding, a new endotherm appeared

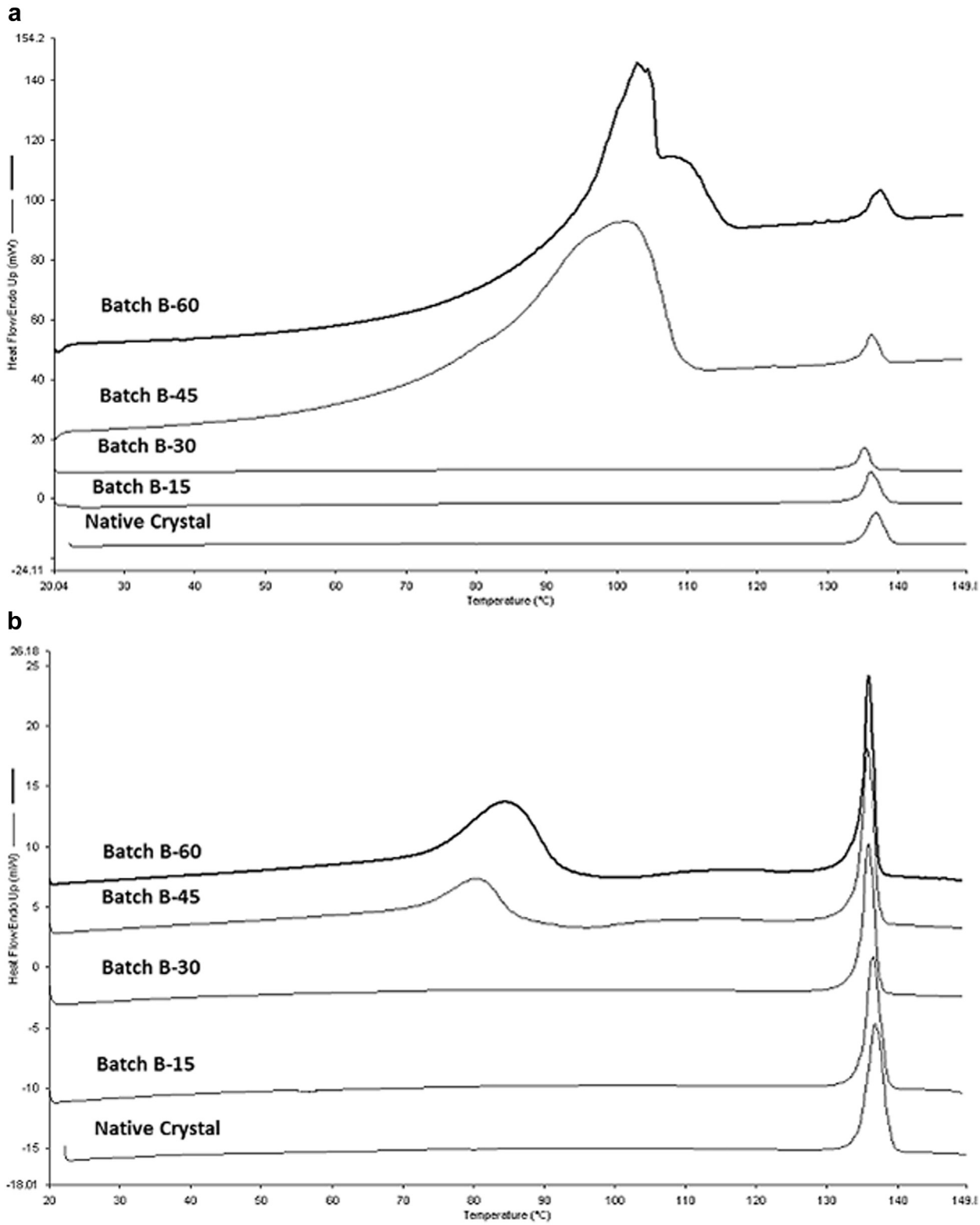


**Figure 9.** Differential scanning calorimetry thermograms of nicergoline ground under Method B: in presence of liquid nitrogen and air atmosphere (60.0 ± 1.0% RH). (a) Analysis run immediately after grinding. (b) Analysis run 5 mo after grinding.

(Table 1) at nearly 118°C-121°C. By comparing the onset temperature information with data in the literature,[1] it is possible to conclude that the endotherm corresponds to the melting of the polymorphic Form II. Between 50°C and 60°C, a slight change in heat capacity could be observed, most probably corresponding to a glass transition.[6] From the DSC results, it is possible to suppose that NCs underwent amorphization under grinding carried out at room conditions and that, during heating in the DSC apparatus, the

**Table 2**
Physicochemical Characterization of Nicergoline Batches Ground Under Method B

| Characteristic | Desolvation Endotherm | | Form I Melting | | Relative Crystallinity Degree | Water Loss |
|---|---|---|---|---|---|---|
| | $T_m$ °C | ΔH J/g | % W/W | ΔH J/g | % | % W/W |
| NCs Form I | – | – | 134.56 ± 0.67 | 63.10 ± 2.54 | 100 | 0.15 ± 0.01 |
| Form II | – | – | 120.34 ± 1.16 | 55.28 ± 1.24 | 100 | 0.35 ± 1.18 |
| Analyzed immediately | | | | | | |
| B-15 | – | – | 133.66 ± 1.24 | 39.97 ± 2.03 | 95 | 0.15 ± 0.01 |
| B-30 | – | – | 133.66 ± 1.05 | 39.87 ± 2.14 | 74 | 0.16 ± 0.02 |
| B-45 | 49.44 ± 3.57 | 1123.09 ± 25.46 | 134.33 ± 0.66 | 24.84 ± 1.27 | – | 5.17 ± 0.11 |
| B-60 | 62.90 ± 4.18 | 1046.11 ± 18.64 | 134.69 ± 0.75 | 21.68 ± 1.89 | – | 5.16 ± 0.15 |
| Analyzed after 5 mo | | | | | | |
| B-15 | – | – | 135.10 ± 0.68 | 57.98 ± 2.18 | 96 | 0.15 ± 0.02 |
| B-30 | – | – | 136.86 ± 1.23 | 56.76 ± 2.65 | 95 | 0.14 ± 0.02 |
| B-45 | 72.12 ± 1.26 | 38.26 ± 2.54 | 133.46 ± 1.15 | 54.26 ± 2.31 | – | 4.49 ± 0.01 |
| B-60 | 72.58 ± 1.15 | 75.72 ± 1.55 | 133.04 ± 1.18 | 54.07 ± 1.19 | – | 5.25 ± 0.01 |

The extrapolated onset temperature ($T_m$) and the melting enthalpy were determined by DSC.
Relative crystallinity degree was determined by XRPD, and the water content % by TGA. Values are the mean of 3 measurements, and standard deviations are indicated.

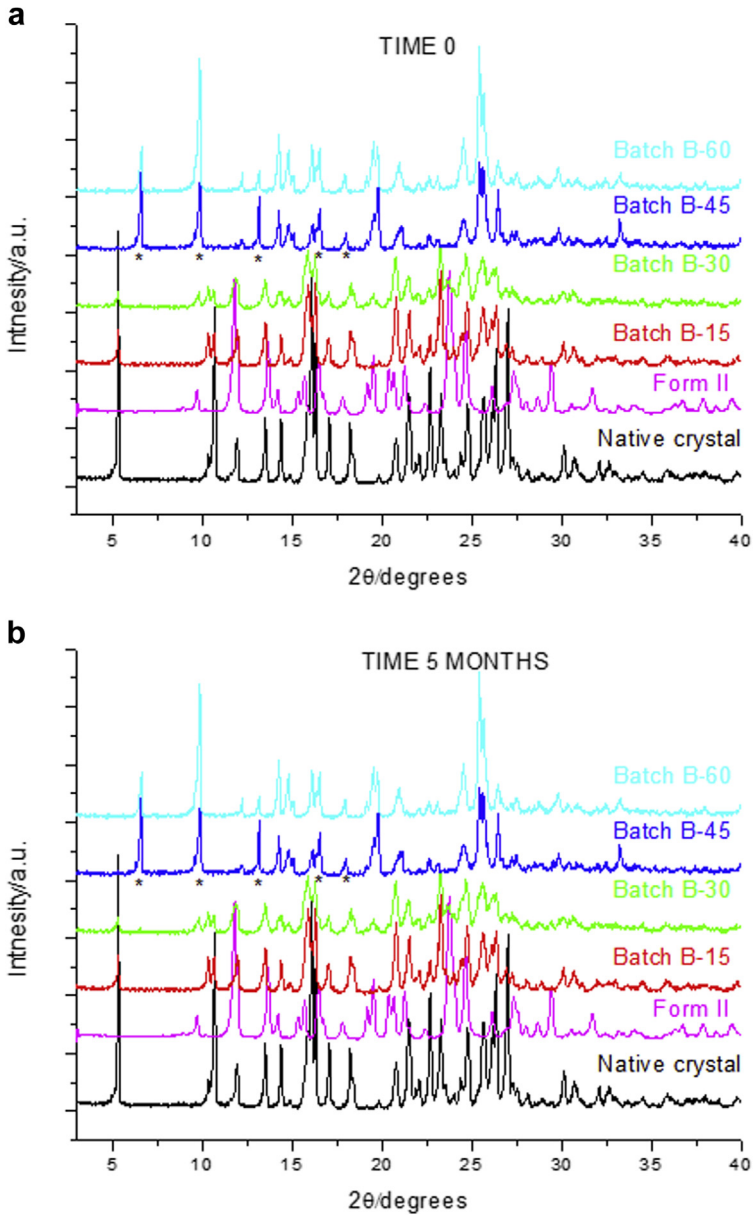


**Figure 10.** X-ray powder diffraction patterns of nicergoline ground under Method B: in presence of liquid nitrogen and air atmosphere (60.0 ± 1.0% RH). (a) Analyses performed immediately after grinding. (b) Analyses performed after 5 mo.

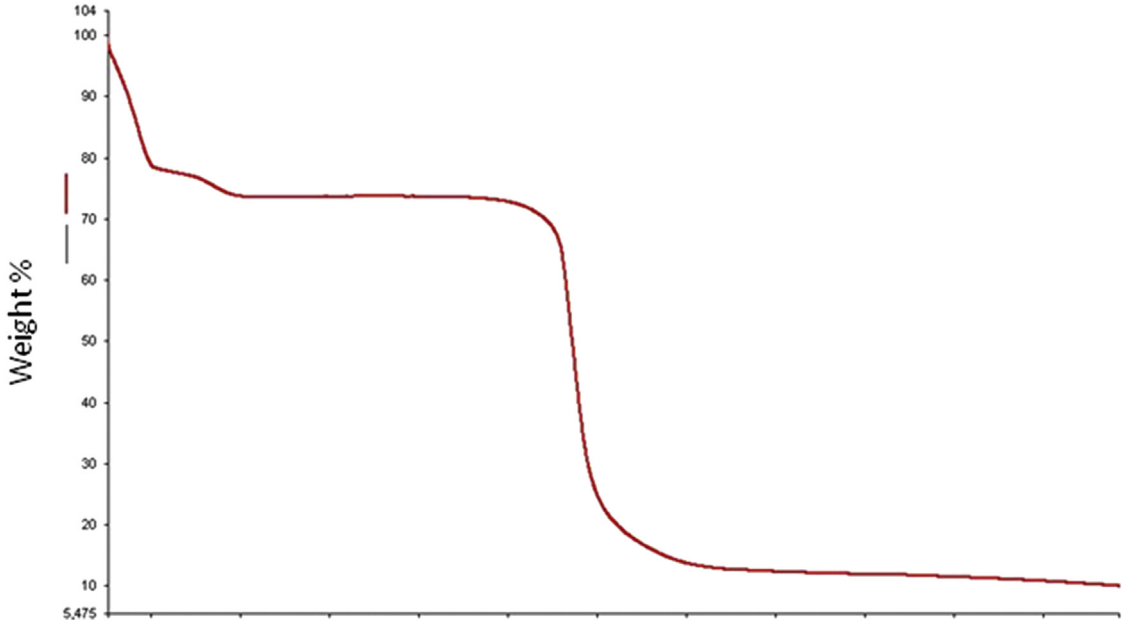


**Figure 11.** TGA thermogram of Batch B-60 run immediately after grinding.

amorphous solid crystallized into the metastable Form II. This phenomenon was observed after at least 30 min of grinding. The nicergoline amorphization can be explained by the fact that it easily amorphizes under different experimental conditions.[6]

The same samples were run again after 1 month and 5 months of storage. In both cases, glass transition was no longer evident, while Form II melting, melt crystallization under Form I, and Form I melting were clearly evident. Figure 4b and Table 1 report only the results after 5 months of storage, because those after 1 month were practically the same. This information confirms the physical stability of these batches during this considered time interval. To confirm the findings from DSC analysis, namely the amorphization of NCs during grinding and the crystallization of the amorphous form under Form II, XRPD was also performed (Fig. 5). There was a progressive decrease in the peak intensity from NCs to Batch A-60, which became somewhat flat in Batches A-45 and A-60. Nevertheless, some peaks were still evident, no change in the peak distances was observed, and no Form II peaks could be highlighted. This demonstrated that during grinding there was a progressive tendency to solid-state amorphization, which justifies the glass transitions observed in DSC thermograms. In conclusion, XRPD confirmed that Batches A-30, A-45, and A-60 were a mix of Form I and amorphous form. Table 1 reports the decrease in crystallinity degree % from 100% to 12%, as calculated by XRPD. Heating in the DSC apparatus promoted the crystallization of the amorphous solid into the metastable Form II, which justifies the presence of the Form II melting endotherm.

XRPD performed on the same Batches after 1 and 5 months of storage at room temperature showed that all the batches crystallized and were a mix of Forms I and II (Fig. 5, Table 1). This means that the amorphous solid crystallized into Form II, which is thermodynamically the most favored form for crystallization of a monotropic system such as that of nicergoline polymorphs[1] under the experimental conditions applied. The crystallinity degrees of batches analyzed after 1 or 5 months were consistent with a completely crystalline solid (Table 1).

The various batches were also analyzed by IR immediately after grinding and subsequently after 1 and 5 months, in order to ascertain whether any kind of modification occurred in the NIC chemical structure. Figure 6 shows no changes in the IR spectra, confirming that no changes in chemical structure occurred under grinding.

The absence of solid hydration was also confirmed by TGA (Table 1): the water content percentage was consistent with an anhydrous solid.

*Method B: Grinding in Presence of Liquid Nitrogen Under Air Atmosphere (60.0 ± 1.0% RH)*

NCs subjected to grinding under Method B showed a progressive particle size reduction (Fig. 7). Particles became increasingly smaller and more rounded; however, a significant agglomeration tendency was evident while grinding proceeded. Figure 8 clearly shows the progressive reduction in particle size while grinding proceeded: moving from NCs to Batch B-60, the particle size distribution was narrower and the 50% cumulative weight was 1.72, 1.20, 0.80, 0.75, and 0.65 μm, respectively, for NCs, Batches B-15, B-30, B-45, and B-60.

DSC analysis performed immediately after grinding showed the appearance of a large endotherm approximately between 40°C and 120°C after 45 and 60 min grinding (Fig. 9a). Because the shape of this curve could be associated with a loss in water, it was hypothesized that the solid hydrated under grinding in presence of liquid nitrogen. The same endotherm was still present after 1 month and 5 months (Fig. 9b), confirming the physicochemical stability of the 2 batches during the interval period considered. XRPD indicated a slight decrease in crystallinity degree after grinding for 15 and 30 min (Table 2, Fig. 10). In addition, no significant change in crystalline structure for batches ground for 30 min could be observed. On the contrary, for Batches B-45 and B-60, a significant change in interreticular distances was observed. New peaks appeared at 6.46, 9.96, 12.20, and 13.90 2θ. In the interval approximately from 2 to 15 2θ, typical peaks of Form I disappeared. At higher distances, peaks of the 2 forms were characterized by similar distances, so it was not possible to clearly distinguish between peaks of the hydrate form and Form I. The diffractograms remained the same 5 months after grinding. Because a change in the crystalline structures occurred, it was not possible to follow the evolution in crystallinity degree during grinding, and thus in Table 2 the crystallinity decrease is only given for Batches B-15 and B-30.

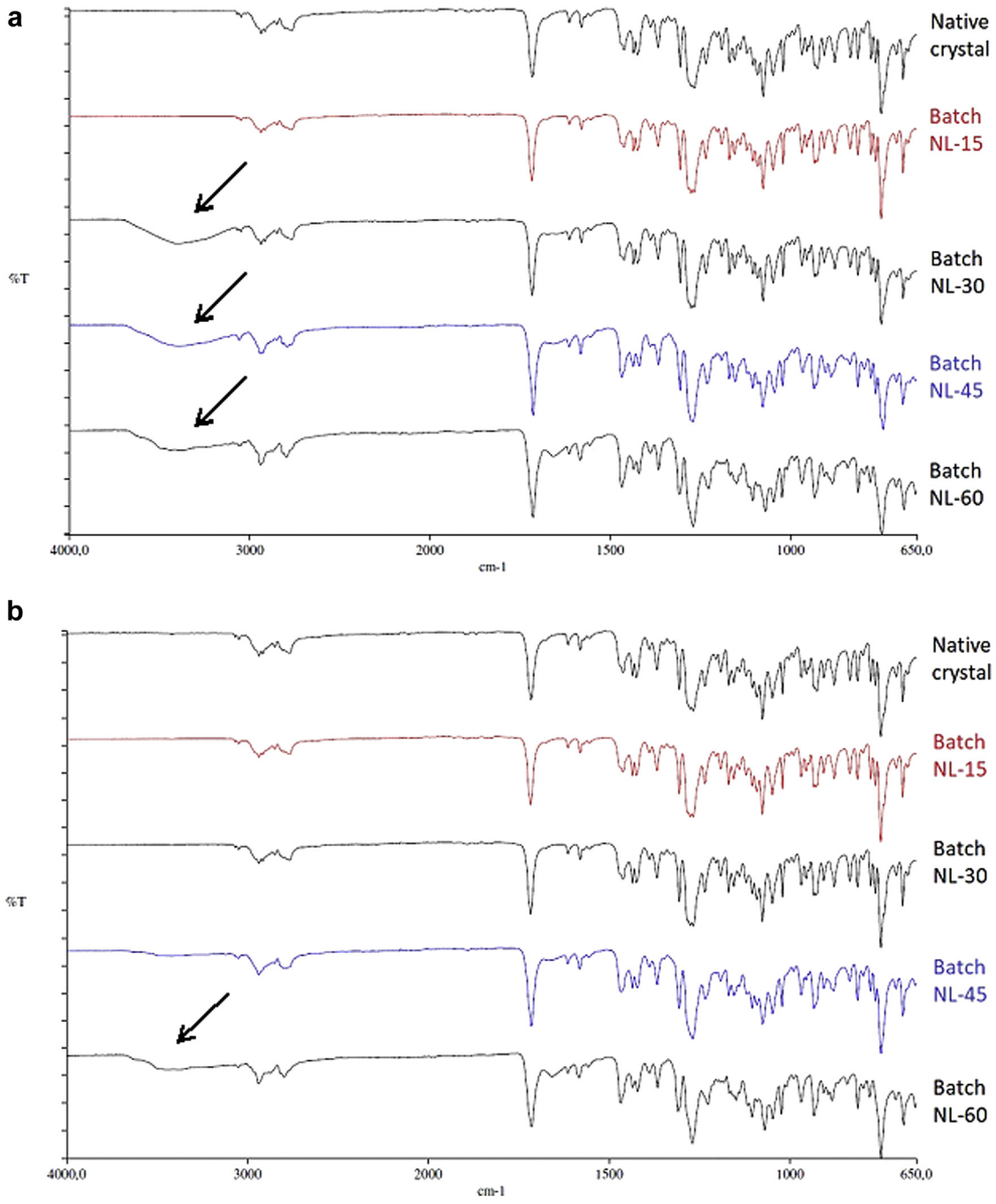


**Figure 12.** Infrared spectroscopy of nicergoline ground under Method B: in presence of liquid nitrogen and air atmosphere (60.0 ± 1.0% RH). (a) Analyses performed immediately after grinding. (b) Analyses performed after 5 mo.

The confirmation of a change in weight was possible by TGA. In Figure 11, a weight decrease was observed from starting temperature to approximately 40°C, corresponding to the loss of absorbed water. From 40°C to 100°C, a further decrease in weight was observed, probably corresponding to desolvated water. Further decrease in weight occurred at nearly 260°C, corresponding to nicergoline decomposition. TGA permitted the calculation of water desolvation (nearly 5.0% W/W), confirming that the DSC endotherm corresponded to dehydration and that changes in inter-reticular distances were in line with the presence of a different form. Calculation of the water loss established the loss of 1 water molecule per NIC molecule, thus a monohydrate is formed during grinding.

The presence of bound water was also confirmed by IR spectroscopy: IR spectra showed a broad band at nearly 3000-3500 $cm^{-1}$, corresponds to the O-H stretching for self-associated water that may be loosely bound (Fig. 12).[26]

In conclusion, it is clearly evident that grinding nicergoline in presence of liquid nitrogen favors solid hydration. It is possible that liquid nitrogen crystallized the surrounding water (present in the surrounding atmosphere, which is 60.0 ± 1.0% RH) that could come into contact with the solid. The energy transferred during grinding, as well as defects produced in the solid under grinding, favored the interaction between NIC and water.

The formation of a hydrate between NIC and water has not been reported in the literature to date.

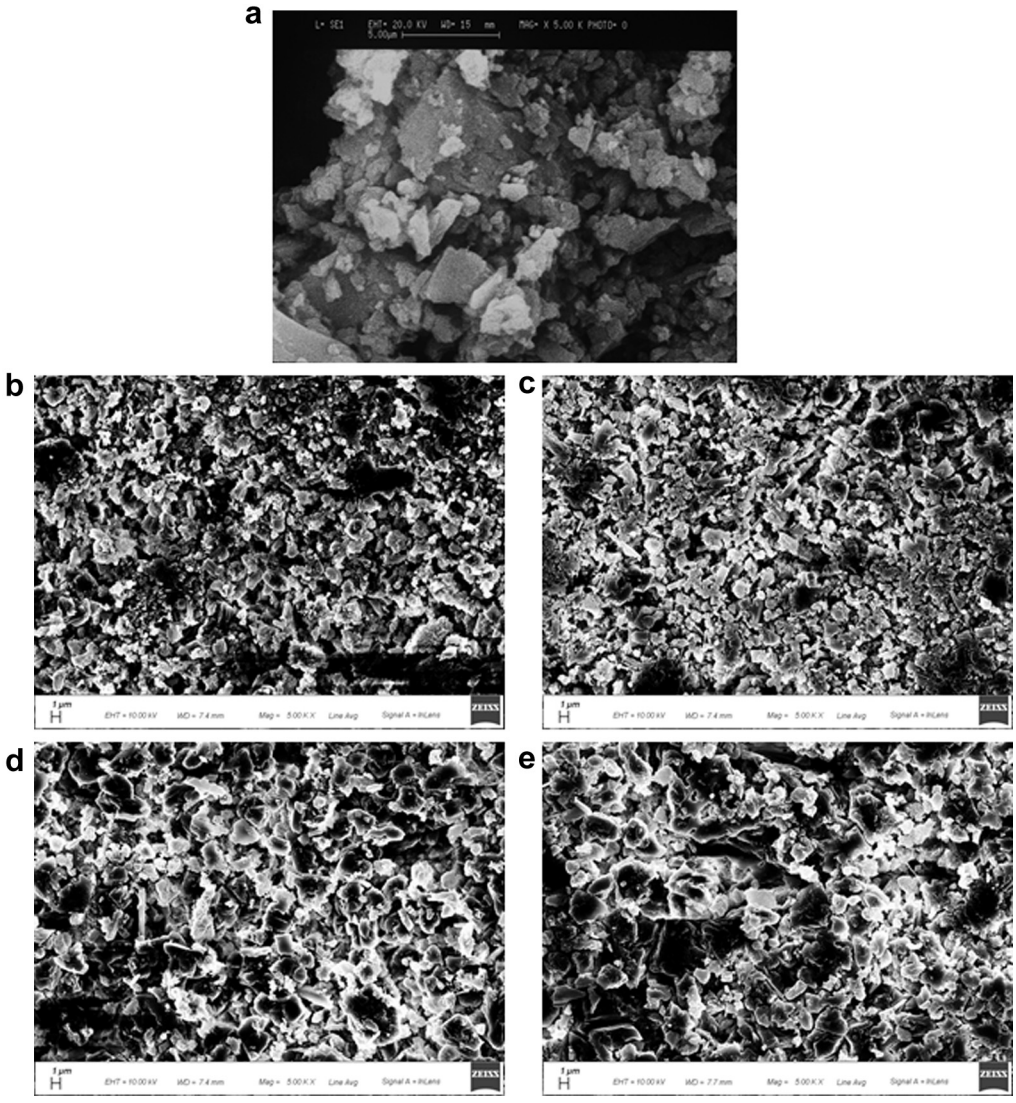


**Figure 13.** Scanning electron photomicrographs of nicergoline ground under Method Method C: 20°C under nitrogen atmosphere (60.0 ± 1.0% RH). Native Crystals (a), Batch C-15 (b), Batch C-30 (c), Batch C-45 (d) and Batch C-60 (e). Magnification of 5000 ×.

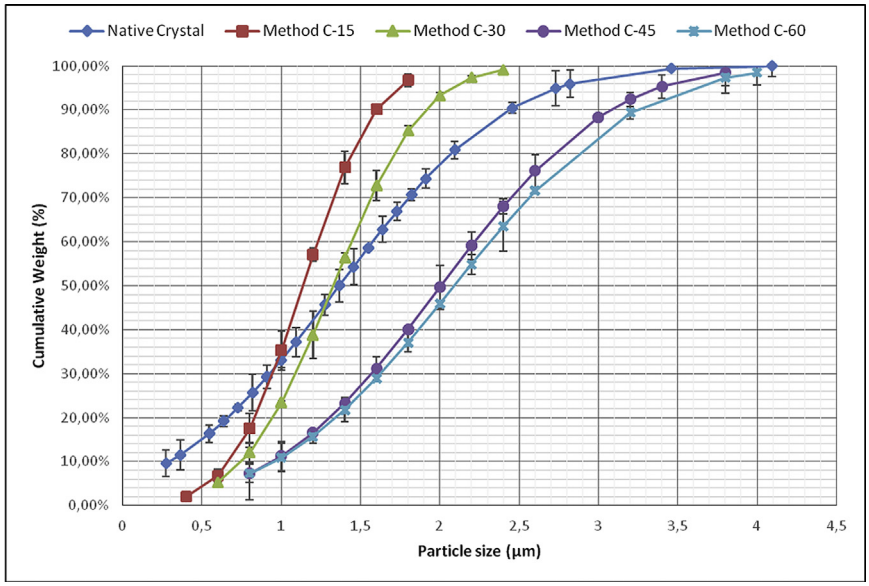


**Figure 14.** Particle size distribution profile of nicergoline ground under Method C: 20°C under nitrogen atmosphere (5.0 ± 1.0% RH). Standard Deviations are indicated.

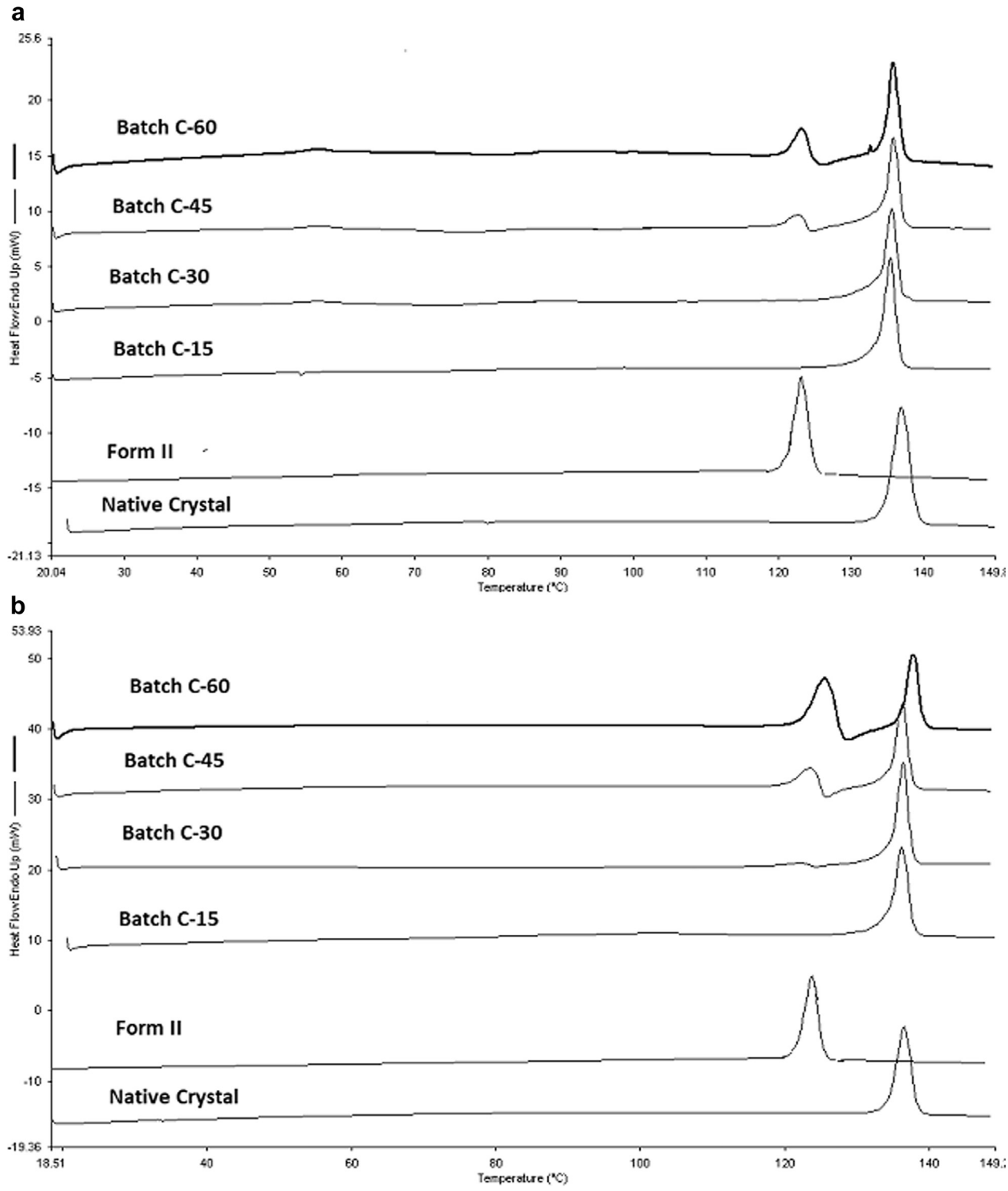


**Figure 15.** Differential scanning calorimetry thermograms of nicergoline ground under Method C: 20°C under nitrogen atmosphere (5.0 ± 1.0% RH). (a) Analysis run immediately after grinding. (b) Analysis run 1 mo after grinding.

Our group previously reported crystal hydration of acyclovir under grinding in presence of liquid nitrogen.[27] In this case, we attributed our finding to the microenvironmental conditions (the presence of water dispersed in air that condenses in presence of liquid nitrogen) together with the grinding, which can perturb the crystals. Of note, the hydrate form of acyclovir crystallized from the anhydrous one under grinding and both forms shared the same monoclinic form, which can explain in structural terms how similar crystal structures can favor the transition from 1 crystal form to another one. We also described hydration during grinding for sodium naproxen.[28] In this case, 2 dihydrate forms and 1 tetrahydrate form were subjected to grinding in presence of liquid nitrogen, during which the progressive hydration to superior hydrates (pentahydrate and hexahydrate) was observed. Sodium naproxen, described as a channel hydrate, demonstrated the ability to accommodate one or more molecules in tunnels formed in the crystal structure. The conclusions of those

**Table 3**
Physicochemical Characterization of Nicergoline Batches Ground Under Method C

| Characteristic | Glass Transition | | Form II Melting | | Form I Melting | | Relative Crystallinity Degree | Water Loss |
|---|---|---|---|---|---|---|---|---|
| | $T_g$ °C | ΔCp J/KG* °C | $T_m$ °C | ΔH J/g | $T_m$ °C | ΔH J/g | % | W/W % |
| NCs Form I | – | – | – | – | 134.56 ± 0.67 | 63.10 ± 2.54 | 100 | 0.15 ± 0.01 |
| Form II | – | – | 120.34 ± 1.16 | 55.28 ± 1.24 | – | – | 100 | 0.35 ± 1.18 |
| Analyzed immediately | | | | | | | | |
| C-15 | – | – | – | – | 133.76 ± 0.44 | 51.79 ± 2.56 | 95 | 0.15 ± 0.02 |
| C-30 | 49.96 ± 0.79 | 100 ± 10 | 118.57 ± 0.22 | 1.80 ± 1.45 | 134.81 ± 0.33 | 53.79 ± 3.24 | 60 | 0.14 ± 0.02 |
| C-45 | 52.04 ± 0.55 | 700 ± 10 | 120.27 ± 0.32 | 6.87 ± 1.37 | 134.27 ± 0.70 | 43.60 ± 3.00 | 38 | 0.14 ± 0.02 |
| C-60 | 52.80 ± 0.22 | 730 ± 10 | 120.87 ± 0.45 | 12.40 ± 2.24 | 134.35 ± 0.28 | 39.03 ± 2.84 | 22 | 0.13 ± 0.02 |
| Analyzed after 5 mo | | | | | | | | |
| C-15 | – | – | – | – | 133.75 ± 0.18 | 51.19 ± 2.35 | 98 | 0.14 ± 0.01 |
| C-30 | – | – | 119.67 ± 0.56 | 6.07 ± 2.11 | 134.39 ± 0.47 | 48.45 ± 2.02 | 99 | 0.13 ± 0.01 |
| C-45 | – | – | 120.65 ± 0.21 | 15.45 ± 1.34 | 134.19 ± 0.11 | 44.99 ± 3.04 | 100 | 0.15 ± 0.02 |
| C-60 | – | – | 120.87 ± 0.16 | 27.80 ± 3.24 | 134.17 ± 0.20 | 36.64 ± 2.78 | 100 | 0.14 ± 0.01 |

The extrapolated onset temperature ($T_m$) and the melting enthalpy were determined by DSC.
Relative crystallinity degree was determined by XRPD, and the water content % by TGA. Values are the mean of 3 measurements, and standard deviations are indicated.

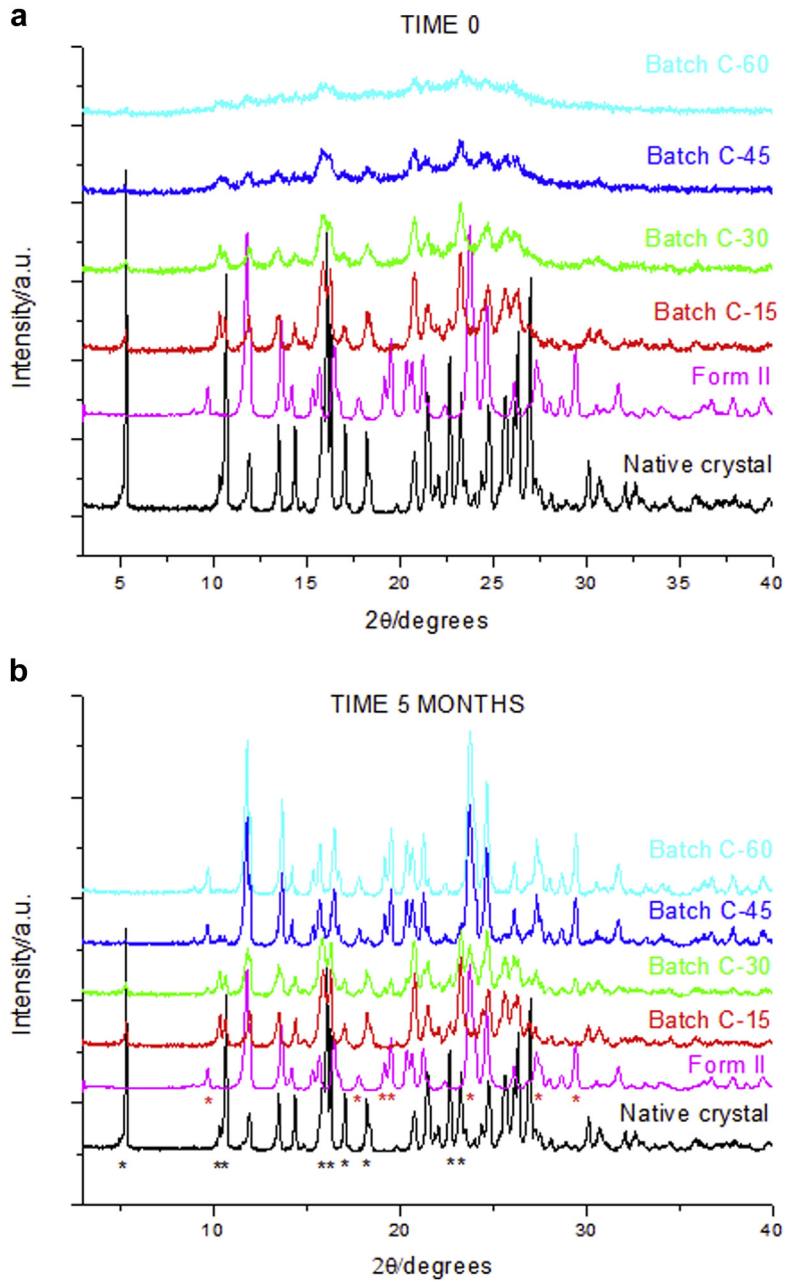


**Figure 16.** X-ray powder diffraction patterns of nicergoline ground under Method C: 20°C under nitrogen atmosphere (5.0 ± 1.0% RH). (a) Analyses performed 1 wk after grinding. (b) Analyses performed after 5 mo.

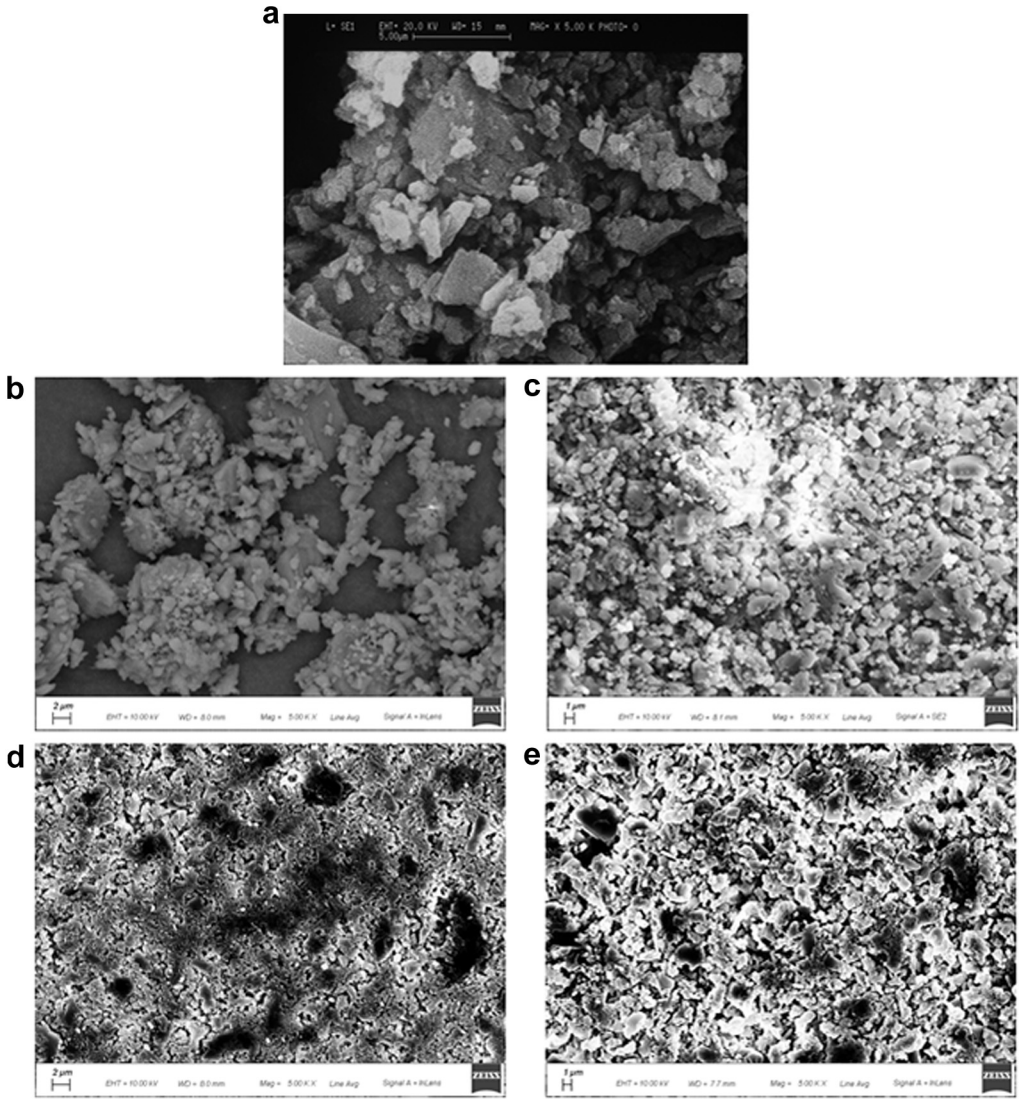


**Figure 17.** Scanning electron photomicrographs of nicergoline ground under Method D: under liquid nitrogen and nitrogen atmosphere (5.0 ± 1.0% RH). Native Crystals (a), Batch D-15 (b), Batch D-30 (c), Batch D-45 (d) and Batch D-60 (e). Magnification of 5000 ×.

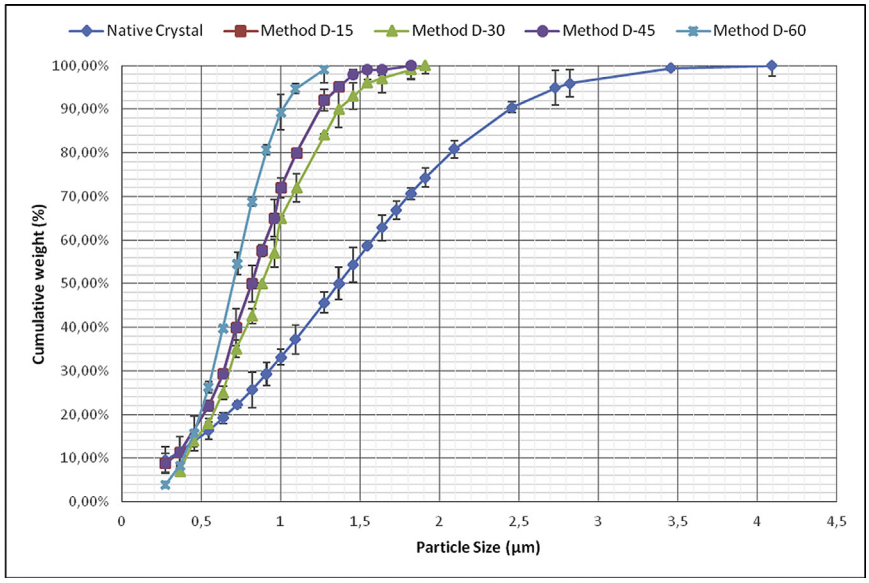


**Figure 18.** Particle size distribution profile of nicergoline ground under Method D: under liquid nitrogen and nitrogen atmosphere (5.0 ± 1.0% RH). Standard deviations are indicated.

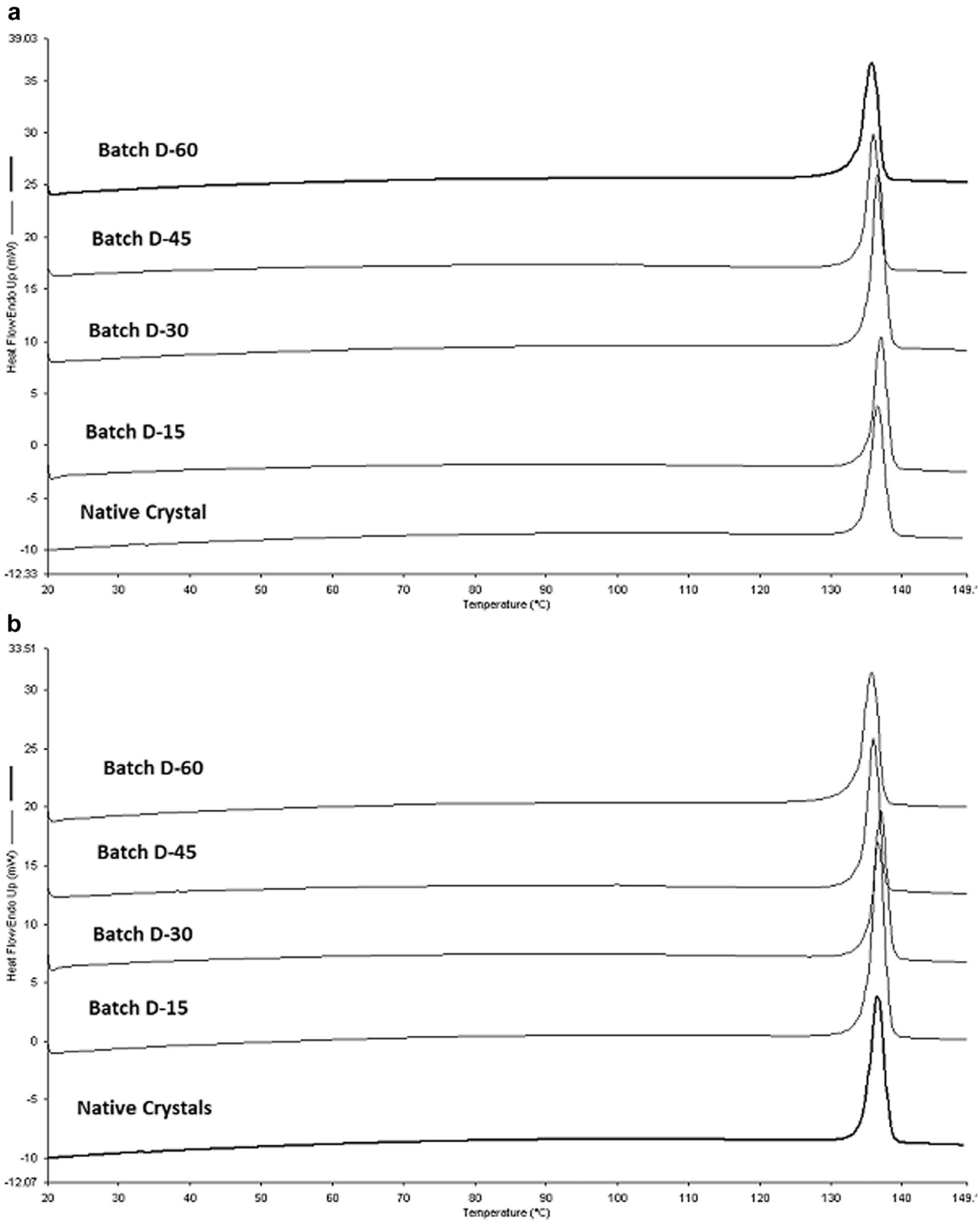


**Figure 19.** Differential scanning calorimetry thermograms of nicergoline ground under Method D: under liquid nitrogen and nitrogen atmosphere (5.0 ± 1.0% RH). (a) Analysis run immediately after grinding. (b) Analysis run 1 mo after grinding.

studies led us to suppose that the anhydrous nicergoline Form I and the monohydrate can share similar crystalline structure. In further studies, we will try to establish the crystallographic structure of the nicergoline monohydrate.

*Method C: Grinding at 20°C Under Nitrogen Atmosphere (5.0 ± 1.0% RH)*

Figure 13 illustrates the strong tendency to particle size reduction; in fact, as early as after 15 min of grinding, there was a significant reduction in particle size. Particles appeared rather rounded

**Table 4**
Physicochemical Characterization of Nicergoline Batches Ground Under Method D

| Characteristic | Form I Melting | | Relative Crystallinity Degree | Water Loss |
|---|---|---|---|---|
| | $T_m$ °C | ΔH J/g | % | W/W % |
| NCs Form I | 134.56 ± 0.67 | 63.10 ± ±2.54 | 100 | 0.16 ± 0.01 |
| NCs Form I | 134.56 ± 0.67 | 63.10 ± 2.54 | 100 | 0.16 ± 0.01 |
| Analyzsed immediately | | | | |
| D-15 | 134.88 ± 0.11 | 54.16 ± ±2.47 | 98 | 0.12 ± 0.01 |
| D-30 | 134.64 ± 0.24 | 51.49 ± ±3.00 | 98 | 0.20 ± 0.01 |
| D-45 | 134.12 ± 0.50 | 49.81 ± ±3.02 | 94 | 0.10 ± 0.02 |
| D-60 | 133.80 ± 0.33 | 41.09 ± ±3.11 | 94 | 0.18 ± 0.02 |
| Analyzsed after 5 mo | | | | |
| D-15 | 134.93 ± 0.25 | 54.97 ± ±2.56 | 98 | 0.15 ± 0.02 |
| D-30 | 135.30 ± 0.37 | 52.86 ± ±2.43 | 98 | 0.15 ± 0.01 |
| D-45 | 134.35 ± 0.12 | 52.82 ± ±2.30 | 94 | 0.16 ± 0.01 |
| D-60 | 133.63 ± 0.64 | 50.34 ± ±2.71 | 94 | 0.16 ± 0.02 |

The extrapolated onset temperature ($T_m$) and the melting enthalpy were determined by DSC.
Relative crystallinity degree was determined by XRPD, and the water content % by TGA. Values are the mean of 3 measurements, and standard deviations are indicated.

after grinding and a strong tendency to particle agglomeration was evident. Figure 14 confirms this observation and illustrates a decrease in particle interval from 0.2 to 4 μm for NCs, to approximately 0.5-1.8 μm and 0.6-2.4 μm for batch C-15 and C-30, respectively. But curiously, with increases in grinding time, there was a sort of agglomeration ("particle fusion") that led to an increase in particle size (Figs. 13 and 14). In this case, the 50% cumulative weight moved from 1.72 μm for NCs to nearly 2.0 μm for batches C-45 and C-60. During the previous grinding methods, individual agglomerated particles could be detected by SEM and measured through the software. But in this case, it was not possible to distinguish individual particles, and thus we refer to a sort of "particle fusion," rather than agglomeration, that led to a more pronounced and close particle aggregation. DSC thermograms (Fig. 15) appeared to be very close to those previously described for Batches ground under Method A: heating the different batches immediately after grinding at 30, 45, and 60 min produced a glass transition, which means that during grinding the solid undergoes amorphization. Heating promoted crystallization into metastable Form II, as proven by the presence of the endotherm corresponding to the Form II melting. The melt crystallized into Form I, which in turn melted (Table 3). Thermograms of batches stored for 1 and 5 months revealed the solid crystallization of amorphous solid under Form II, as proven by the absence of the glass transition and the presence of the melting endotherm of the metastable Form II (Table 3).

DSC results were confirmed by XRPD. Diffractograms of batches ground for 30, 45, and 60 min and immediately analyzed revealed amorphization, and after 1 and 5 months of storage the amorphous solid crystallized into the metastable Form II (Fig. 16). Thus, in these XRPD diffractograms, no amorphous part could be noted, while a change in the peak distances was observed, with patterns corresponding to a mix of Form II and Form I crystals. TGA revealed a low water content and a weight loss % compatible with an anhydrous solid (Table 3), while IR analysis revealed the chemical stability of the solid, as the spectra were unchanged compared to those of native crystals.

*Method D: Grinding in the Presence of Liquid Nitrogen Under Nitrogen Atmosphere (5.0 ± 1.0% RH)*

Figure 17 shows a strong tendency to particle size reduction; as early as after 15 min of grinding, particles were very small. They appeared as small irregular particles with rather smooth edges. During grinding, a strong tendency to particle agglomeration could be observed.

The efficiency in particle size reduction under this method is illustrated in Figure 18, which shows a significant particle size reduction after only 15 min of grinding. An increase in grinding time did not correspond to a significant further decrease in particle size.

DSC analysis (Fig. 19) revealed the great physicochemical stability of nicergoline under Method D: no changes in thermograms could be seen during grinding and no change was observed for batches stored for 1 and 5 months (Table 4).

XRPD confirmed the DSC results (Fig. 20) and no changes in inter-reticular distances were observed during grinding, even if a certain decrease in crystallinity degree could be noticed (Table 4). No changes were observed in crystallinity degree after 5 months of storage. The physicochemical stability was also proven by IR spectroscopy and TGA analysis (Table 4).

NCs ground under Method D thus behaved differently than those ground under Method B. In the former case, the presence of nitrogen gas prevented the condensation of water into the grinding environment, which instead would be favored by the liquid nitrogen. The presence of the inert gas actually blocked the interaction of nicergoline and water, hindering the nicergoline hydration.

*Intrinsic Dissolution Rate and Particle Dissolution*

The IDR and particle dissolution were compared for NCs and Batches A-60, B-60, C-60, and D-60 stored for 1 month. The intrinsic dissolution rate (Table 5), which is known to be influenced by the crystalline form but not by the particle size, showed that the worst IDR was exhibited by the hydrate (Batch B-60), while NCs showed intermediate behavior, and the best was exhibited by Batches B-60 and C-60 because of the presence of Form II, which, as already shown in previous studies, exhibited higher dissolution than Form I. The highest IDR of metastable Form II is in line with the monotropic thermodynamic relationship between Form I and II.[1]

The hydrate showed the worst IDR, in line with Khankari and Grant,[29] who reported that the solubility and thus the dissolution rates of hydrates are worse than those of the parent forms.[29-31]

Dissolution experiments were carried out in presence of sodium laureth sulfate to minimize the effect of particle agglomeration. The particle size dissolution (Fig. 21) reflected in part not only the evidence from the intrinsic dissolution results but also the evidence from the particle size. The slowest were crystals of Form I, not subjected to any particle size reduction. Thus, the dissolution behavior reflected the effect of crystalline form and large particle size. The best dissolution rate was seen for the particles ground under Method D (Batch D-60). This result mainly reflected the great reduction in particle size and to a minor extent the fact that Form I is crystalline. The particle dissolution results of Batch A-60 and Batch C-60 were lower than those of Batch D-60.

One would expect batches A-60 and C-60, which contain in part Form II, to have better particle dissolution, especially if

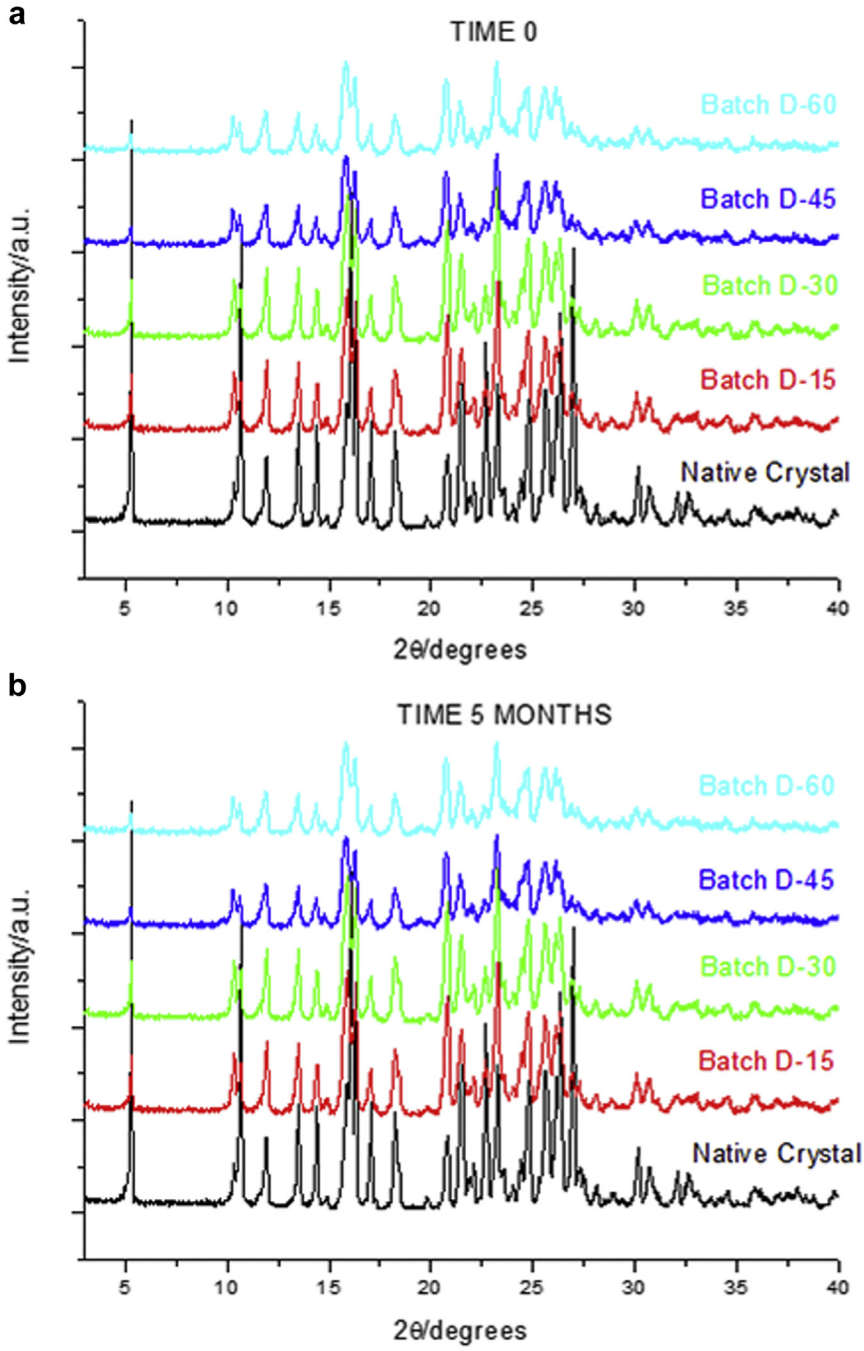


**Figure 20.** X-ray powder diffraction patterns of nicergoline ground under Method D: under liquid nitrogen and nitrogen atmosphere (5.0 ± 1.0% RH). The analyses were performed immediately after grinding.

one considers that these batches also have the best IDR. However, this was not the case, perhaps because of the effect of particle size and thus particle surface area exposed to the dissolution medium. In addition, batch C-60 exhibited a faster dissolution rate than batch A-60 because of its smaller particle size.

**Table 5**
Intrinsic Dissolution Rates of Different Nicergoline Samples

| Variable | Slope/g $l^{-1}min^{-1}$ | R | IDR/mol $min^{-1}$ $Mm^{-2}$ |
|---|---|---|---|
| Form I (native crystals) | 0.0290 | 0.9982 | 4.5132E-7 |
| Batch A-60 | 0.0321 | 0.9992 | 4.9922E-7 |
| Batch B-60 (Monohydrate form) | 0.0102 | 0.9998 | 1.5863E-7 |
| Batch C-60 | 0.0322 | 0.9997 | 5.0078E-7 |
| Batch D-60 | 0.0297 | 0.9995 | 4.6190E-7 |

Intrinsic dissolution rates (IDR) were calculated from the slope of dissolution curves determined during the first 20 min of dissolution.

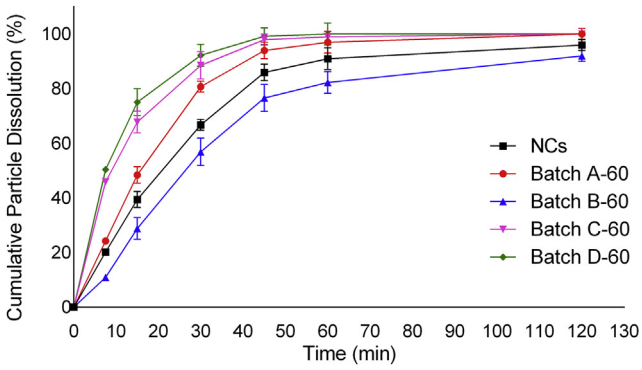


**Figure 21.** Particle dissolution of nicergoline from different batches.

Undissolved solids in solutions prepared for parallel dissolution experiments were removed and examined by XRPD for changes in crystalline form: results showed that no changes in crystalline form occurred during dissolution for any batch.

## Conclusions

The particle dissolution of coarser crystals can be improved under grinding, but the physicochemical characteristics of powders obtained under different grinding conditions must be carefully monitored in order to avoid unexpected solid-solid transition, which can even worsen particle dissolution.

This is the case of nicergoline in this study. It showed unexpected hydration when ground in presence of liquid nitrogen and air atmosphere; the hydration promoted a significant decrease in IDR, which negatively impacted particle dissolution.

We found that this negative effect can be avoided simply by performing the grinding of nicergoline under nitrogen gas. This method yielded very small particle size and prevented conversion to the hydrate and Form II, assuring good physicochemical stability during the drug shelf life and avoiding unexpected solid-state transition.

## Acknowledgments

The authors would like to thank Laura Petetta for her contribution to SEM analysis and Sheila Beatty for editing the English usage of the manuscript.

The authors also acknowledge receipt of funding from the European Commission of an H2020-MSCA-ITN-2015 award through the ISPIC project (grant number 675743) and an H2020-MSCA-RISE-2016 award through the CHARMED project (grant number 734684).

## References

1. Malaj L, Censi R, Capsoni D, et al. Characterization of nicergoline polymorphs crystallized in several organic solvents. *J Pharm Sci*. 2011;100(7):2610-2622.
2. Hušák M, Had J, Kratochvíl B, Cvak L, Stuchlík J, Jegorov A. X-ray absolute structure of nicergoline (form I). Quantitative analysis of nicergoline phase mixture: form I/form II. *Collect Czech Chem Commun*. 1994;59(7):1624-1636.
3. Foresti E, Sabatino P, Riva di Sanseverino L, Fusco R, Tosi C, Tonani R. Structure and molecular orbital study of ergoline derivatives. 1-(6-Methyl-8β-ergolinylmethyl) imidazolidine-2, 4-dione (I) and 2-(10-methoxy-1, 6-dimethyl-8β-ergolinyl) ethyl 3, 5-dimethyl-1H-2-pyrrolecarboxylate toluene hemisolvate (II) and comparison with nicergoline (III). *Acta Crystallogr B Struct Sci*. 1988;44(3):307-315.
4. Husak M, Kratochvil B, Ondracek J, Maixner J, Jegorov A, Stuchlik J. The crystal and absolute molecular structure of "low melting" nicergoline (form II). *Z Fur Kristallogr*. 1994;209:260-262.
5. Censi R, Martena V, Hoti E, Malaj L, Di Martino P. Preformulation study of nicergoline solid dispersions. *J Therm Anal Calorim*. 2014;115(3):2439-2446.
6. Martena V, Censi R, Hoti E, Malaj L, Di Martino P. Physicochemical characterization of nicergoline and cabergoline in its amorphous state. *J Therm Anal Calorim*. 2012;108(1):323-332.
7. Martena V, Censi R, Hoti E, Malaj L, Di Martino P. A new nanospray drying method for the preparation of nicergoline pure nanoparticles. *J Nanopart Res*. 2012;14(6):934.
8. Khadka P, Ro J, Kim H, et al. Pharmaceutical particle technologies: an approach to improve drug solubility, dissolution and bioavailability. *Asian J Pharm Sci*. 2014;9(6):304-316.
9. Liversidge GG, Cundy KC. Particle size reduction for improvement of oral bioavailability of hydrophobic drugs: I. Absolute oral bioavailability of nanocrystalline danazol in beagle dogs. *Int J Pharm*. 1995;125(1):91-97.
10. Hickey AJ, Ganderton D. *Pharmaceutical process engineering*. In: *Drugs and the Pharmaceutical Science*. 112. New York, NY: Marcel Dekker; 2001:174-197.
11. Joshi JT. A review on micronization techniques. *J Pharm Sci Technol*. 2011;3:651-681.
12. Brunaugh A, Smyth H. Process optimization and particle engineering of micronized drug powders via milling. *Drug Deliv Transl Res*. 2018;8(6):1740-1750.
13. Martena V, Censi R, Hoti E, Malaj L, Di Martino P. Preparation of glibenclamide nanocrystals by a simple laboratory scale ultra cryo-milling. *J Nanopart Res*. 2013;15(6):1712.
14. Niwa T, Nakanishi Y, Danjo K. One-step preparation of pharmaceutical nanocrystals using ultra cryo-milling technique in liquid nitrogen. *Eur J Pharm Sci*. 2010;41(1):78-85.
15. Zanolla D, Perissutti B, Passerini N, et al. Milling and comilling Praziquantel at cryogenic and room temperatures: assessment of the process-induced effects on drug properties. *J Pharm Biomed Anal*. 2018;153:82-89.
16. Gubskaya AV, Lisnyak YV, Blagoy YP. Effect of cryogrinding on physicochemical properties of drugs. I. Theophylline: evaluation of particles sizes and the degree of crystallinity, relation to dissolution parameters. *Drug Dev Ind Pharm*. 1995;21(17):1953-1964.
17. Sugimoto S, Niwa T, Nakanishi Y, Danjo K. Development of a novel ultra cryo-milling technique for a poorly water-soluble drug using dry ice beads and liquid nitrogen. *Int J Pharm*. 2012;426(1-2):162-169.
18. Crowley KJ, Zografi G. Cryogenic grinding of indomethacin polymorphs and solvates: assessment of amorphous phase formation and amorphous phase physical stability. *J Pharm Sci*. 2002;91(2):492-507.
19. Di Martino P, Magnoni F, Vargas Peregrina D, Rosa Gigliobianco M, Censi R, Malaj L. Formation, physicochemical characterization, and thermodynamic stability of the amorphous state of drugs and excipients. *Curr Pharm Des*. 2016;22(32):4959-4974.
20. Zhang GG, Law D, Schmitt EA, Qiu Y. Phase transformation considerations during process development and manufacture of solid oral dosage forms. *Adv Drug Deliv Rev*. 2004;56(3):371-390.
21. Hasa D, Jones W. Screening for new pharmaceutical solid forms using mechanochemistry: a practical guide. *Adv Drug Deliv Rev*. 2017;117:147-161.
22. Lin S-Y. Mechanochemical approaches to pharmaceutical cocrystal formation and stability analysis. *Curr Pharm Des*. 2016;22(32):5001-5018.
23. Roberts KJ, Docherty R, Tamura R. *Engineering Crystallography: From Molecule to Crystal to Functional Form*. Dordrecht, Netherlands: Springer; 2017.
24. Gashi Z, Censi R, Malaj L, et al. Differences in the interaction between aryl propionic acid derivatives and poly (vinylpyrrolidone) K30: a multimethodological approach. *J Pharm Sci*. 2009;98(11):4216-4228.
25. Banakar U. Factors that influence dissolution testing. In: *Pharm Dissolution Testing*. 49. Boca Raton, FL: CRC Press; 1992:151-155.
26. Zhu H, Padden BE, Munson EJ, Grant DJ. Physicochemical characterization of nedocromil bivalent metal salt hydrates. 2. Nedocromil zinc. *J Pharm Sci*. 1997;86(4):418-429.
27. Magnoni F, Gigliobianco MR, Peregrina DV, Censi R, Di Martino P. Effect of grinding on the solid-state stability and particle dissolution of acyclovir polymorphs. *J Pharm Sci*. 2017;106(10):3084-3094.
28. Malaj L, Censi R, Martino PD. Mechanisms for dehydration of three sodium naproxen hydrates. *Cryst Growth Design*. 2009;9(5):2128-2136.
29. Khankari RK, Grant DJ. Pharmaceutical hydrates. *Thermochim Acta*. 1995;248:61-79.
30. Blagden N, de Matas M, Gavan PT, York P. Crystal engineering of active pharmaceutical ingredients to improve solubility and dissolution rates. *Adv Drug Deliv Rev*. 2007;59(7):617-630.
31. Shan N, Zaworotko MJ. Polymorphic crystal forms and cocrystals in drug delivery (crystal engineering). In: *Burger's Medicinal Chemistry and Drug Discovery*. Hoboken, NJ: John Wiley & Sons Inc.; 2010.